PROBING THE INTERIOR OF VOLCANIC PLUMES WITH W AND L-BAND RADIATION

A Thesis
Presented to
The Academic Faculty

By

Joshua Méndez

In Partial Fulfillment
of the Requirements for the Degree
Masters in Science in the
School of Electrical and Computer Engineering

Georgia Institute of Technology

December 2017

PROBING THE INTERIOR OF VOLCANIC PLUMES WITH W AND L-BAND RADIATION

Approved by:

Dr. Paul Steffes
School of Electrical and Computer Engineering
Georgia Institute of Technology

Dr. Gregory Durgin
School of Electrical and Computer Engineering
Georgia Institute of Technology

Dr. Josef Dufek
School of Earth and Atmospheric Science
Georgia Institute of Technology

Date Approved: January 11, 2000

"Definitely something inside there, but all scans are being reflected back."

–Unnamed Lieutenant, *Star Trek: The Motion Picture*, 1979

To my grandparents, Esperanza y Daniel

ACKNOWLEDGEMENTS

I would like to thank:

My advisor, Paul Steffes for his guidance, academic freedom, and support these last 4 years

The NSF GRFP and Blue Waters Fellowship programs

My committee: Greg Durgin and Josef Dufek

The Steffes Group: Alex Akins and Amadeo Bellotti

Other mentors: (GT) Josef Dufek, Carol Paty, James Wray, Louis Boulanger, Scott Elliot, and James Steinberg. (BU) Ted Fritz, Mark Horenstein, Paul Hall, Bob Kingsland, Malay Mazumder, Colleen Dalton, and Tommaso Toffoli

Friends at GT and Atlanta: Francesco Amato, Hansel Enriquez, Jaime Convers, Ke Qi, Kyle Xu, Steven Mitchell, Gregory Karahalis

Val and Chris Harper, who have been second parents to me these past 10 years

George McDonald for his unwavering support, wisdom, and kindness

My parents, who, despite the distance, have always been by my side. A mis padres, quienes a pesar de la distancia, siempre han estado a mi lado.

TABLE OF CONTENTS

LIST OF TABLES

LIST OF FIGURES

LIST OF SYMBOLS

$< P >$	Average power loss
$\alpha(R)$	Attenuation coefficient
ϵ_0	Permittivity of free space
ϵ_r'	Imaginary part of the relative permittivity
ϵ_r'	Real part of the relative permittivity
η	Surface charge density
γ_{factor}	Constant equal to 0.1
$\hbar$	Reduced Plank constant
λ	Wavelength
$\mathbf{K}$	Surface current density
$\mathbf{u}$	Surface charge carrier velocity
μ_0	Relative permeability of space
μ_1	Relative permeability of particle
ω	Angular frequency
ϕ	Surface potential
$\psi_n(\rho)$	Ricatti-Bessel function of the first kind
σ_s	Phenomenological surface conductivity
$\tilde{\epsilon}$	Complex relative permittivity
$\tilde{m}$	Complex refractive index
$\xi_n(\rho)$	Ricatti-Bessel function of the third kind
a_n	Scattering coefficient
b_n	Scattering coefficient

C_{abs} Scattering cross-section

C_{ext} Extinction cross-section

C_{sca} Scattering cross-section

D Particle diameter

E Electric field

e Electron charge

E_s Stored energy in the resonator

f_0 Resonant frequency

H Magnetic field

$HPBW$ Half-power bandwidth

k_B Boltzmann constant

k_C Coulomb's constant

m' Real part of the index of refraction

m'' Imaginary part of the index of refraction

m_e Electron mass

N_T Total number of particles per unit volume

Q_m Quality factor for a lossy media

Q_{abs} Absorption efficiency

Q_{ext} Extinction efficiency

Q_{factor} Quality factor

Q_{sca} Scattering efficiency

R Particle radius

T Temperature

x Size parameter

SUMMARY

Probing the interior dynamics of eruptive columns using electrostatic processes generated within the flows themselves has garnered much interest in the recent years [Arason et al., 2011; Behnke et al., 2012; James et al., 1998; Méndez Harper et al., 2016; Miura et al., 1996; Thomas et al., 2009]. Indeed, large eruptions are often accompanied by brilliant displays of lightning, testifying to the high potentials that can be accumulated by a diverse set of electrification mechanisms. Unfortunately, lightning on its own cannot be used as a general remote sensing tool because not all volcanic eruptions produce spark discharges. As pointed out by McNutt et al., 2010, only 30-35% of volcanoes maintain lightning storms. The absence of lightning in two thirds of all eruptions indicates that most volcanoes produce flows with 1) inefficient or limited granular charging processes or 2) dynamics that do not promote the charge separation that sets up coherent electric fields needed for lightning. Yet, even if the prerequisites for spark discharges are not met, it is difficult to argue for plumes which are completely electrostatically neutral. The problems permeating passive electromagnetic sensing may be overcome through the use of active methods which involve interrogating charged volcanic plumes with electromagnetic radiation. The scattering of electromagnetic waves has been a common method to retrieve the physical properties of collections of particles, specifically those which cannot be accessed directly. In the present work, we numerically and experimentally explore the manner in which electrostatic charge on particles affects the propagation of electromagnetic waves through volcanic plumes. We show that, for the range of complex dielectric constants measured in volcanic ash, the extinction efficiency of a charged particle is significantly larger than that associated with an equivalent neutral particle for L-band radiation. Conversely, we find that charging on sub-millimeter-sized particles does not directly affect the propagation of W-band radiation. However, we find that changes to the dynamics of a particle system resulting from charging can be detected indirectly with millimeter-wave light. Thus, this

work represents the first effort to characterize how electomagnetic radiation can be used to assess charging in volcanic plumes.

CHAPTER 1
INTRODUCTION AND BACKGROUND

1.1 Charging in volcanic plumes

Direct sampling of near-vent volcanic jets is difficult, costly, and dangerous. However, understanding the granular dynamics in this region is critical to determine the long-term behavior of a volcanic flow (i.e. will the jet rise buoyantly into the atmosphere or collapse to produce pyroclastic density currents). Thus, developing tools to probe the interior of plumes remotely and rapidly is of paramount importance. One avenue that has much garnered interest in the last 20 years is the possibility of studying of volcanic clouds through electrostatic mechanisms [James et al., 1998; McNutt et al., 2010; Méndez Harper et al., 2016; Van Eaton et al., 2016]. A recent review study found that 27-35 % of eruptions were accompanied by lightning, suggesting the presence of highly-efficient charge generation and separation mechanisms within plumes [McNutt et al., 2010]. These mechanisms include triboelectrification [Cimarelli et al., 2014; Forward et al., 2009b], fragmentation charging [James et al., 2000; Méndez Harper et al., 2015], and charging related to the nucleation of hydrometeors [Arason et al., 2011; Nicora et al., 2013]. Because electromagnetic signals associated with charging can be detected from afar, changes in the ambient field as well as impulsive lightning signals can be used to monitor eruptions remotely and in poor weather conditions [James et al., 1998] (see Figure 1.1).

The effort to link hydrodynamics to electrostatic phenomena in volcanic plumes has a history spanning more than a century. Pioneering field investigations were performed by Symons et al. [1888], Hatakeyama [1947], and Nagata et al. [1948] who observed changes in the electric field during large eruptions and spark discharges. In the laboratory, experiments on triboelectrification were conducted by Hatakeyama et al. [1951] who described

Figure 1.1: Volcanic lightning is a common phenomenon during eruptions. Spark discharges in the dusty, volcanic plume can range from a few meters to kilometers. Because volcanic lightning produces signals that can be detected from afar, electrostatic processes during eruptions may lead to novel methods to interrogate plumes remotely.

the charging of particles from the Aso and Asama volcanoes. Their experiments were the first to observe particle-size-sensitive charging phenomena in a volcanic material. More recently, similar experiments were conducted by Kikuchi et al. [1982] using Mt. Usu ash; these authors observed a similar size effect. The charge on particles has also been directly measured in the field by Gilbert et al. [1991] and Miura et al. [1996], who found that grains could be electrified to potentials approaching the theoretical maximum (27 μC m^{-2}). In the last decade, triboelectric charging of ash in a simulated conduit was explored by Cimarelli et al. [2014], who demonstrated that frictional and collisional charging alone can result in the production of discharges. Houghton et al. [2013] also found a correlation between the particle size distribution of an ash sample and the amount of charging. In the field, Thomas et al. [2007] has shown that volcanic lightning can be categorized in three modalities: vent lightning (comprising visibly-imperceptible discharges at the vent), near-vent lightning (discharges several 10s to 100s of meters in length occurring in the transition between the jet-thrust region and the plume), and plume lightning (large-scale lightning occurring at elevation in the plume. Behnke et al. [2015] demonstrated that these forms of lightning develop at different time within the eruption suggesting they are controlled by specific eruption parameters. Furthermore, research efforts in the industrial sector suggest that the electrification of granular materials is strongly dependent on the dynamics of the flow. Similar links between plume kinematics and electrostatics have recently been identified during eruptions of Augustine, Redoubt, and Sakurajima [Behnke et al., 2013; Cimarelli et al., 2016; Thomas et al., 2007]. At both Augustine (2006) and Redoubt (2009), for example, a marked change in electrical activity was detected using a Lightning Mapping Array when the initial explosive phase of the eruption gave way to a buoyantly rising plume [Behnke et al., 2015, 2013; Thomas et al., 2007]. Furthermore, observations at these volcanoes revealed three distinct forms of lightning, occurring at different times and within specific regions of the plumes. At Sakurajima, the frequency of discharges observed in jets was found to correlate with the overpressure magnitude at the vent (as inferred from

infrasound) [Aizawa et al., 2016; Cimarelli et al., 2016]. While both volcanologists and atmospheric scientists agree that plume dynamics and electrification are related, quantitative models describing how these two processes are linked have yet to be developed.

1.2 Characterizing charged volcanic plumes actively using electromagnetic waves

Up until this point electrostatic phenomena in plumes have been studied almost exclusively using passive methods, either by monitoring changes in the ambient electric field or capturing the radio frequency bursts radiated during lightning stokes. While such procedures have revealed a great deal about the manner in which volcanic flows become electrified, they have important limitations that hinder their ability to be used universally. Firstly, as aforementioned, only 27-35 % of eruptions generate spark discharges, meaning that electrostatic processes can be studied at less than half of all active volcanoes with tools like the Lightning Mapping Array. Volcanic plumes that do not produce lightning are not necessarily uncharged, but likely charged to degrees that to not exceed the breakdown threshold for air. These *undersaturated* plumes have been studied using a broad suite of electrostatic sensors including field mills, slow antennas, and Langmuir-type probes (e.g Harrison et al. [2010] and Miura et al. [2002]), but such instruments produce data which can be difficult to interpret. Furthermore, the electric field falls off with the square of distance, meaning that sensors must be placed in close proximity to the vent. Lastly, the electric fields in the plume may be masked by ions collected at the surface of the granular flow. In the present work, we argue that many of the limitations discussed above can be bypassed using *active* remote sensing techniques. A number of authors have recently shown through Mie theory that charged particles can importantly impact the propagation of electromagnetic waves. Namely, for certain combinations of particle size and wavelength, charged particles can increase the attenuation significantly relative to the neutral particles. The fundamental framework relating to the attenuation due to charged particles finds its origin in the work of Bohren et al. [1977]. These authors described how classical Mie theory could be modified

to account for charge trapped on the surface of particles. More recently, Klačka et al. [2007] provided the exact mathematical solution to the problem, showing that charged particles can affect electromagnetic waves if the particles are 2 to 3 orders of magnitude smaller than the illuminating wavelength. In some fields, especially those relating to communications, the effects of charged particles on the propagation of micro and millimeter-wave are considered problematic. Yet, other investigators have realized the value of being able to characterize the charged grains from the manner in which they attenuate light. For instance, Heinisch et al. [2012] have explored the possibility of studying charged astrophysical grains through the anomalous extinction of infrared frequencies. Similarly, Kocifaj et al. [2015] have proposed that increased backscatter of millimeter waves from thunderclouds could be used to gauge the probability of lightning. Here, we consider the viability of applying similar principles to charged volcanic plumes and other geophysical flows. While (given the brevity of a master's thesis) the results present herein should be considered preliminary, our results do emphasize the fact that active methods of characterizing charged granular systems are extremely promising and should be pursued to greater lengths.

1.3 Organization

This thesis is organized as follows: Chapter 2, through application of the modified Mie theory described above, explores the degree to which charging in volcanic plumes can attenuate electromagnetic waves. In particular, we explore under what conditions ubiquitous GPS signals (L-band) can be used to characterize, or at least detect, electrification in volcanic flows. We compare our results to the limited existing field data. Chapter 3 experimentally investigates the effects of fluidized charged particles on the propagation of W-band (75-110 GHz) radiation using a Fabry-Perot resonator. Chapter 4 describes on-going efforts to experimentally validate the numerical modeling delineated in Chapter 1. Such study makes use of a custom-made coaxial probe. Finally, Chapter 5 includes concluding remarks.

CHAPTER 2

PROBING CHARGED VOLCANIC PLUMES USING GPS

This chapter is currently being formated for submission to Geophysical Research Letters as Méndez Harper, J., Steffes, P., and Dufek, J. *Probing charged volcanic plumes using GPS*

2.1 Introduction

Volcanic eruptions can loft large amounts of ash into the atmosphere, producing hazards to both aircraft and near-by populations. Furthermore, suspended material may have long-lasting effects on climate. While determining the spatial and temporal behaviors of large plumes remains an prime objective of scientists and governments, studying the interior dynamics of these granular flows is technically challenging and costly. Thus, a need for tools that can retrieve data remotely exists within the volcanological community. One avenue that has garnered substantial attention over the last two decades involves probing the interior dynamics of eruptive columns using electrostatic processes generated within the flows themselves [Aizawa et al., 2016; Behnke et al., 2015; James et al., 1998; Kikuchi et al., 1982; Miura et al., 1996; Thomas et al., 2007]. Indeed, large eruptions are often accompanied by brilliant displays of lightning, testifying to the high potentials that can be accumulated by a diverse set of electrification mechanisms (including fractoemission, triboelectrification, and electrification processes similar to those found in thunderstorms) [Cimarelli et al., 2014; Kikuchi et al., 1982; Méndez Harper et al., 2015, 2016]. Beyond signals at optical wavelengths, volcanic lightning generates a wide array of electromagnetic signals that can be recorded from afar. We note that the idea of studying granular flows through electrostatic phenomena did not arise from the geophysical community, but has been a goal long pursued by those in the industrial, pharmaceutical, and agricultural sectors [Forward et al., 2009a; Lacks et al., 2007, 2011]. While only a few dedicated stud-

ies of volcanic lightning exist, such endeavors have demonstrated that discharge processes are highly sensitive to changes in the kinematics of volcanic flows [Aizawa et al., 2016; Behnke et al., 2015, 2013; Cimarelli et al., 2016; Thomas et al., 2007]. Unfortunately, lightning on its own cannot be used as a general remote sensing tool because not all volcanic eruptions produce spark discharges. As pointed out by McNutt et al. [2010], only 30-35 $\%$ of volcanoes maintain lightning storms. The absence of lightning in two thirds of all eruptions indicates that most volcanoes produce flows with 1) inefficient or limited granular charging processes or 2) dynamics that do not promote the charge separation that sets up coherent electric fields needed for lightning. Yet, even if the prerequisites for spark discharges are not met, it is difficult to argue for plumes which are completely electrostatically neutral. Triboelectrification (encompassing both frictional and contact charging), for instance, will remain active as long as particle-particle collisions exist within a plume [Forward et al., 2009b; Méndez Harper et al., 2016; Pahtz et al., 2010]. Indeed, even surfaces that gently osculate may become electrified triboelectrically [Apodaca et al., 2010]. Furthermore, charged-undersaturated flows still generate signals that can be monitored at a distance. Thus, a worthwhile objective is to find methodologies to effectively exploit these more subtle electromagnetic cues. A straightforward, passive procedure to characterize plumes with low degrees of electrification involves measuring the change in the ambient electric fields produced by the granular flows. Such approach has been used by at Aso [Hatakeyama, 1947; Hatakeyama et al., 1951], and Sakurajima [Miura et al., 1996] using instruments such as field mills and slow antennas. Yet, these approaches suffer from important limitations. Firstly, the electric field generated by a plume may be obscured or shielded by that of free ions which become attracted to the flow's boundary. Secondly, unlike the impulsive signals produced by lightning, the slow-varying electric fields generated by the charged plume fall off rapidly with distance, severely constraining measurement geometries. Lastly, inverting the charge structure of a plume from electric fields with a high resolution would require a large number of sensors, resulting in an increasingly complex

operation. The problems permeating passive electromagnetic sensing may be overcome through the use of active methods which involve interrogating charged volcanic plumes with electromagnetic radiation. The scattering of electromagnetic waves has been a common method to retrieve the physical properties of collections of particles, specifically those which cannot be accessed directly [Bohren et al., 2008; Hulst, 1957]. However, standard Mie-Lorenz-Debye theory [Mie, 1908] implicitly assumes that particles carry no excess charge through the condition of the magnetic field at the boundary between the surrounding medium and the particle:

$$\mathbf{n}\times(\mathbf{H}_2 - \mathbf{H}_1) = 0 \tag{2.1}$$

or the electric displacement boundary condition:

$$\mathbf{n}\cdot(\mathbf{D}_2 - \mathbf{D}_1) = 0. \tag{2.2}$$

However, Bohren et al. [1977] indicate that the boundary conditions can be modified to include the effects of surface charge as:

$$\mathbf{n}\times(\mathbf{H}_2 - \mathbf{H}_1) = \mathbf{K}, \tag{2.3}$$

$$\mathbf{n}\times(\mathbf{E}_2 - \mathbf{E}_1) = 0. \tag{2.4}$$

Above, $\mathbf{K}$ is the surface current density equal to $\sigma_s\mathbf{E}_{1,T}$ where σ_s is the phenomenological surface conductivity and $\mathbf{E}_{1,T}$ is the tangential component of the electric field. Starting from this theoretical framework, Klačka et al. [2007] showed that surface charge may influence the extinction properties of grains if such particles have diameters, D , significantly smaller than the wavelength of the incident radiation, λ. Specifically, for size parameters, $x = D\pi/\lambda$, smaller than ≈ 0.01 charged grains may attenuate electromagnetic radiation an order of magnitude more efficiently than their neutral counterparts. Based on this model, Kocifaj et al. [2015] has suggested that charging in thunderclouds could be as-

sessed by detecting anomalous backscatter. We posit that the properties of charged volcanic plumes could likewise be studied using robust, existing radio frequency infrastructure–the Global Positioning System. Recently, GPS signals, which fall within the L-band of the radio spectrum ($\lambda = 0.30 - 0.15$ m), have been shown to be influenced by the presence of volcanic plumes [Aranzulla et al., 2013; Houlié et al., 2005; Larson, 2013; Larson et al., 2017]. However, as noted by Larson et al. [2017], it is difficult to reconcile the reduction in signal-to-noise ratios of GPS signals propagating through the plumes with the attenuation expected from ash and ice alone. One possibility is that charging in these plumes is responsible for the large dips in SNR observed at volcanoes such as Etna and Redoubt. In the present work, we numerically explore the manner in which charge on particles affect the propagation of electromagnetic waves through volcanic plumes. We show that, for the range of complex dielectric constants measured in volcanic ash, the extinction efficiency of a charged particle is more than one order of magnitude larger than that associated with an equivalent neutral particle. Thus, this work describes a novel method to explore charging in volcanic plumes.

2.2 Theory and Methods

The present endeavor finds its source in the classic work of Mie [1908]. Fascinated by the colorful effects associated with colloidal gold solutions, Gustav Mie presented a way to compute scattering by small particles using Maxwell's electromagnetic theory. Today, his theory finds applications in a wide range of fields, from astrophysics to plasmonics [Eaton, 1984; Lal et al., 2007; Rowe et al., 2008]. However, Mie only characterized the scattering of electrically neutral particles–that is, particles carrying no excess charge on their surfaces. Such limitation has been alleviated, however, by the work of Bohren et al. [1977] and Klačka et al. [2007] who modified Mie coefficients to include the effects of charge. According to Mie theory, the scattering C_{sca} , absorption C_{abs}, and the total

extinction C_{ext} cross-sections are given as:

$$C_{ext} = \frac{2\pi}{k^2} \sum_{n=1}^{\infty} (2n+1) Re(a_n + b_n) \tag{2.5}$$

$$C_{sca} = \frac{2\pi}{k^2} \sum_{n=1}^{\infty} (2n+1)(|a_n|^2 + |b_n|^2); \tag{2.6}$$

$$C_{abs} = C_{ext} - C_{sca}. \tag{2.7}$$

Alternatively, efficiency factors–that is, the cross-sections defined above normalized to a particle's geometrical cross-section–can be expressed as $Q_{abs} = C_{abs}/(\pi R^2)$, $Q_{sca} = C_{sca}/(\pi R^2)$, and $Q_{ext} = C_{ext}/(\pi R^2)$. The modified boundary conditions in equations 2.3 and 2.4 lead to the following scattering coefficients a_n and b_n:

$$a_n = \frac{A_{1n}\psi_n(x) - A_{2n}\psi_{n-1}(x)}{A_{1n}\xi_n(x) - A_{2n}\xi_{n-1}(x)} \tag{2.8}$$

$$b_n = \frac{B_{1n}\psi_n(x) - \psi_{n-1}(x)}{B_{1n}\xi_n(x) - \xi_{n-1}(x)}, \tag{2.9}$$

where

$$A_{1n} = (1 + \frac{ng}{x}) D_n(\tilde{m}x) + \frac{\tilde{m}n}{x} \frac{\mu_o}{\mu_1} \tag{2.10}$$

$$A_{2n} = \tilde{m} \frac{\mu_o}{\mu_1} + g D_n(\tilde{m}x) \tag{2.11}$$

$$B_{1n} = \tilde{m} \frac{\mu_o}{\mu_1} D_n(\tilde{m}x) + \frac{n}{x} - g \tag{2.12}$$

$$g = \frac{x}{2} \frac{\omega_s^2}{\omega^2 + \gamma_s^2} \frac{(-1 + i\gamma_s)}{\omega}, \tag{2.13}$$

$$D_n(\tilde{m}x) = \frac{\psi_n'(\tilde{m}x)}{\psi_n(\tilde{m}x)}, \tag{2.14}$$

$$\omega_s^2 = \frac{2e}{m_e} \frac{\phi}{R^2}, \tag{2.15}$$

$$\gamma_s = \gamma_{factor} \frac{k_B T}{\hbar}. \tag{2.16}$$

Above, μ_1 and μ_0 are the relative permeabilities of the the particle and the medium, respectively (here we assume that $\mu_1 = \mu_0$); $\tilde{m}$ is the complex refractive index; $\psi_n(\rho)$ is the Ricatti-Bessel function of the first kind and $\xi_n(\rho)$ is the Ricatti-Bessel of the third kind; R is the particle radius; λ is the wavelength; the non-dimensional size parameter x is defined as the ratio of particle size to the wavelength $2\pi R/\lambda$; m_e and e are the mass and charge of an electron, respectively; k_B is the Boltzmann constant; $\hbar$ is the reduced Plank constant; and T is temperature in Kelvin (here we assume a constant temperature of 273 K). Klacka et al. [2010] propose that $\gamma_{factor} = 0.1$. The square of the plasma frequency (equation 2.15) incorporates the effects of electrification through the potential ϕ:

$$\phi = 4\pi k_C R\eta \tag{2.17}$$

where η is the surface charge density and k_C is Coulomb's constant. One can see that setting $\eta = 0$ reduces equations 2.8 and 2.9 to the classical scattering coefficients. The dielectric properties of products from several volcanoes have been explored by Adams et al. [1996] and Oguchi et al. [2009]. Between 4 and 19 GHz, these authors showed that the relative permittivities of ash are virtually independent of frequency. Similar to the analysis made in Larson et al. [2017], we assume that this invariance holds down to the L-band frequencies of interest. Note that Adams et al. [1996] did find that the magnitude of the real and imaginary components of the relative permittivity decrease with increasing silica content. From the relative permittivity one can compute the complex refraction index as $\tilde{m}^2 = \tilde{\epsilon_r} = \epsilon_r' + j\epsilon_r''$ (as in Bohren et al. [2008], the convention used here utilizes a non-negative imaginary component). The real and imaginary components of the indices of refraction for ash from six volcanoes are listed in table 2.1 (In an attempt to help preserve Native American heritage, we emphasize the use the volcanoes' pre-Columbian names in the present work). A number of experimental and field efforts have attempted to characterize the charge densities acquired by volcanic particles. Gilbert et al. [1991] measured the

Table 2.1: Real and imaginary components of the refractive index for various volcanoes.

Volcano	$\%_0 SiO_2$	ϵ'	ϵ''	m'	m''
Chi Q'aq'(Fuego), Cuauhtemallan	51	5.649	0.084	2.5475	0.0526
Pacaya, Cuauhtemallan	50	5.802	0.107	2.4769	0.0315
K'idazq'eni (Mt. Spurr), USA	56	6.041	0.108	2.4718	0.0275
Gagxanul (Santa Maria), Cuauhtemallan	65	6.109	0.136	2.4579	0.0220
Lawetlat'la (Mt. Saint Helens), USA	68	6.134	0.156	2.4088	0.0222
Atitlan, Cuauhtemallan	76	6.487	0.268	2.3768	0.0177

charge on individual grains falling out of a Sakurajima plume using an electrostatic separator. These investigators found that eruptions could produce particles with maximum charge densities approaching the theoretical limit of 27 μC m^{-2} (not surprisingly, since electrical breakdown processes–lightning–are often seen in plumes). Similar values were obtained by Miura et al. [1996] at the same volcano. Experimentally, James et al. [2000] reported that charge densities on the order of 10^{-8} - $10^{-6.5}$ C m^{-2} were generated during the reduction of pumice samples through either fracture or abrasion. More recently, Mendez Harper et al. [2017] reported charges densities ranging between 10^{-9} - 10^{-6} C m^{-2} on Popocatepetl and Atexcac grains charged triboelectrically. Using these parameters we can compute the extinction cross-sections C_{ext} for single ash particles with diameters ranging between 1 - 10^5 μm (ash- to lapilli-sized pyroclasts). For GPS bands L1 and L2, with wavelengths of 19.5 (1575.42 MHz) and 24.3 cm (1227.60 MHz), respectively, this results in size parameters spanning 10^{-2} - 10^{-1}. Our model is based on the Mie scattering code developed by Schäfer et al. [2012].

2.3 Results and discussion

The effects of surface charge on the spectral characteristics of ash particles can be readily observed by computing the ratio of the efficiency factors for charged particles Q_c to those associated with neutral particles Q. These ratios are rendered in Figure 2.1 as functions of

the size parameter. As a starting point, we assume particles carry charge densities equal to the theoretical maximum value of 27 μC m^{-2}. As can be seen, charge importantly modifies scattering and absorption processes when the size parameter is less than ≈ 0.05. In other words, for the L-band wavelengths considered here, excess surface charge has an impact on the radiative transfer of volcanic particles with radii smaller than ≈ 1000 μm. Having computed the extinction cross-sections, the total path extinction coefficient for radiation traversing a collection of particles can be calculated as:

$$\alpha(R) = C_{ext}(R)N_T \tag{2.18}$$

where N_T is the total number of particles per unit volume. This expression has units of Nepers m^{-1}. For long path-lengths, it is often more useful to give the above quantity in dB km^{-1}; equation 2.18 needs to be multiplied by 4.343×10^3:

$$\alpha(R) = 4.343 \times 10^3 C_{ext}(R)N_T \tag{2.19}$$

For a more realistic cloud containing particles of different diameters, the attenuation coefficient is found as [Dou et al., 2017; Hulst, 1957]:

$$\alpha = 4.343 \times 10^3 \int_{R_{min}}^{R_{max}} C_{ext}(R)N(R)dR. \tag{2.20}$$

Above, R_{min} and R_{max} are the minimum and maximum radii in the particle size distribution, respectively, and N(R)dR is the total number of particles with radii R to $R + dR$ per unit volume. However, for brevity, only the path attenuation from monodisperse particle clouds are computed below for both L1 and L2. These calculations are done for different mass loadings: 1e^{-4}, 0.001, 0.01, and 0.1 kg m^{-3}. Attenuation for L1 are shown in Figure 2.2, while those associated with L2 are rendered in Figure 2.3. In those figures, subplots A render attenuation for the rhyolitic (Atitlan) end-member in Table 2.1, while those dis-

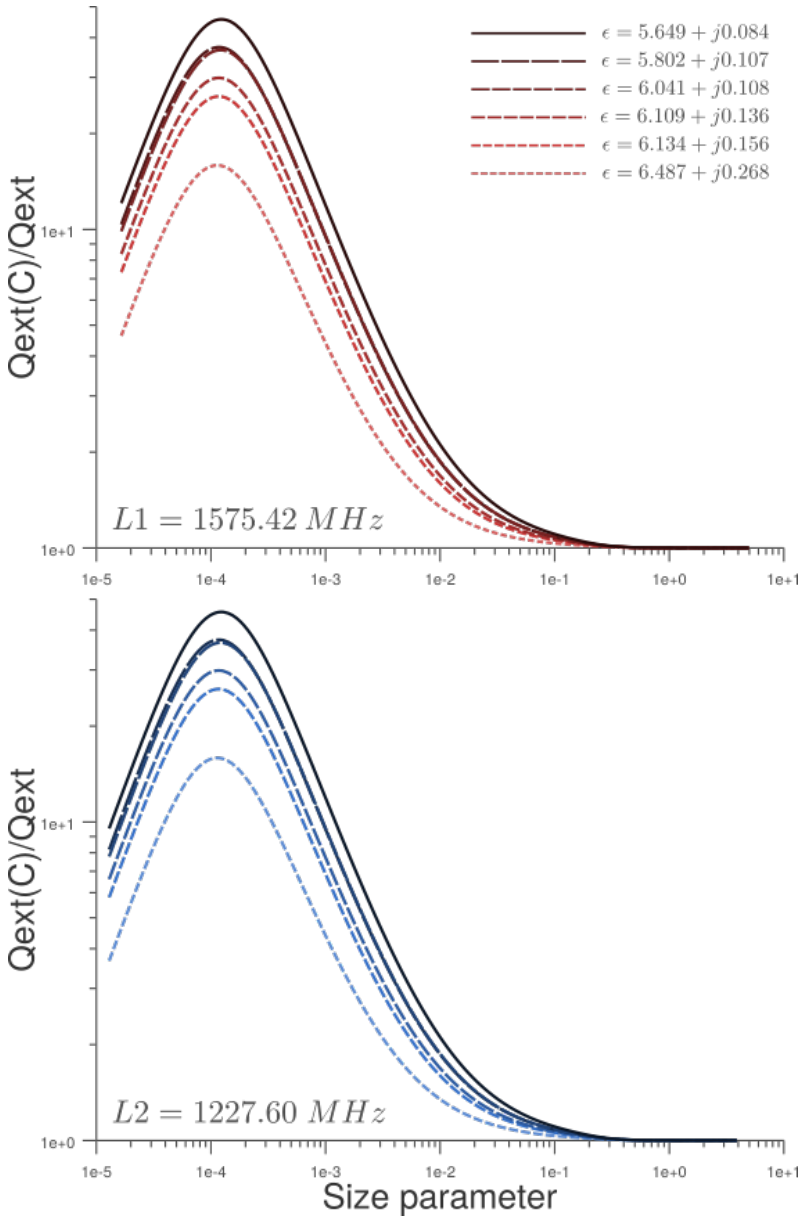

Figure 2.1: Ratio of efficiency factors for charged and non-charged volcanic ash grain as function of size parameter. These ratios are plotted for the samples summarized in Table 2.1. A) L1 = 1575.42 MHz. B) L2 = 1227.60 MHz

played in subplots B are representative of the basaltic compositions (Chi Q'aq'). The key piece of information revealed by Figures 2.2 and 2.3 is that, for a given mass loading, charge on particles in the range of 1 - 1000 microns (i.e. fine to coarse ash) can attenuate L-band signals up to 15 times more effectively than their electrically neutral counterparts. The maximum signal damage occurs when particles are approximately 10 microns in diameter, or when the size parameter is ≈ 0.0001. As particles become larger (> 1000 microns), the attenuation curves for both the charged and uncharged cases converge and attenuation is dominated by scattering rather than absorption. Note that effects of charge on attenuation are highly dependent on silica content, with charged basaltic particles (solid red curves in Figures 2.2B and 2.3B) having greater loss relative to uncharged basaltic particles (blue, dashed curves in Figures 2.2B and 2.3B) than charged rhyolitic ashes relative to uncharged rhyolitic particles (Figures 2.2A and 2.3A). Up until now, we have considered the attenuation of electromagnetic radiation passing through a collection of electrified particles with charge densities at the breakdown limit, 27 μCm^{-2}. While, as mentioned above, elevated charge densities have been measured both experimentally and in the field, most ash particles in plumes are likely undersaturated in charge. Thus, it is instructive to explore how lesser degrees of charging impact the propagation of L-band signals in dusty media. The percent increase in attenuation as a function of charge–that is, $(\alpha_c - \alpha)/\alpha \times 100$–appears in Figure 2.4 A and B for L1 and L2, respectively. This computation was done for charge densities reported in previous work ($\eta = 10^{-8}$ - 10^{-5} Cm^{-2}) [Gilbert et al., 1991; James et al., 2002; Méndez Harper et al., 2016; Mendez Harper et al., 2017]. Important increases in attenuation (larger than 10 $\%$) occur when the charge density is above $\eta = 10^{-7}$ Cm^{-2} and the particle size is smaller than 50 microns. As mentioned previously, Larson et al. [2017] performed first order calculations using the Rayleigh approximation to determine whether ash or hydro-meteors could produce the observed dips in signal-to-noise ratios of GPS data captured during eruptions of the Redoubt and Etna volcanoes. These investigators concluded that the effect of ice can be neglected, while pyroclasts (uncharged ash) may

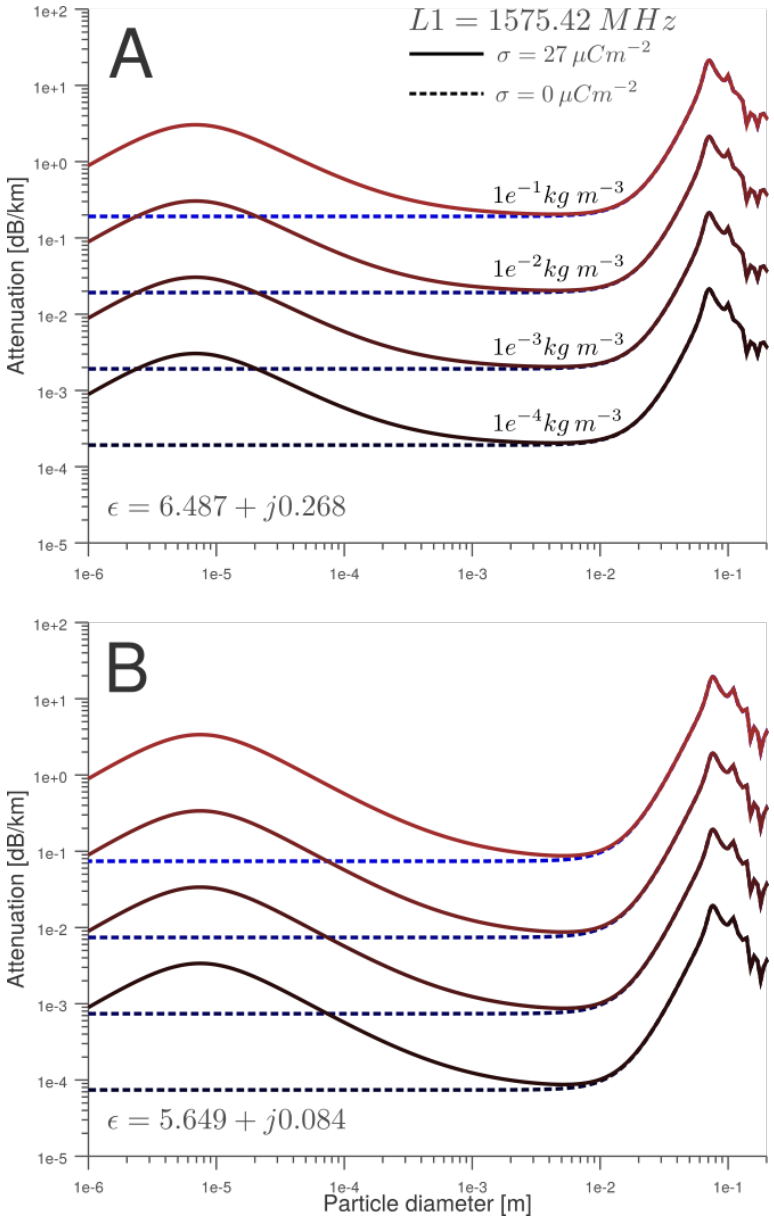

Figure 2.2: Attenuation associated with L1 as a function of particle size for both charged (solid red) and uncharged (dashed blue) particles and for different ash loadings. A) Rhyolite ash. B) Mafic ash.

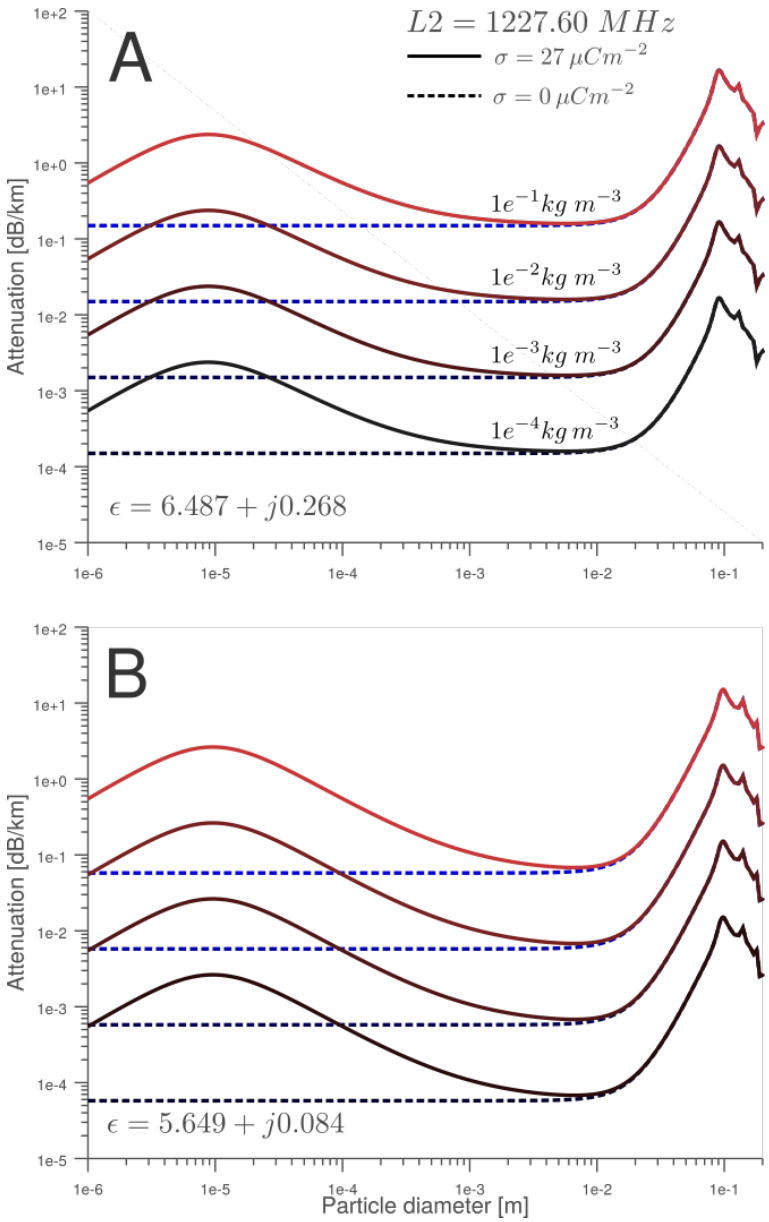

Figure 2.3: Attenuation associated with L2 as a function of particle size for both charged (solid red) and uncharged (dashed blue) particles and for different ash loadings. A) Rhyolite ash. B) Mafic ash.

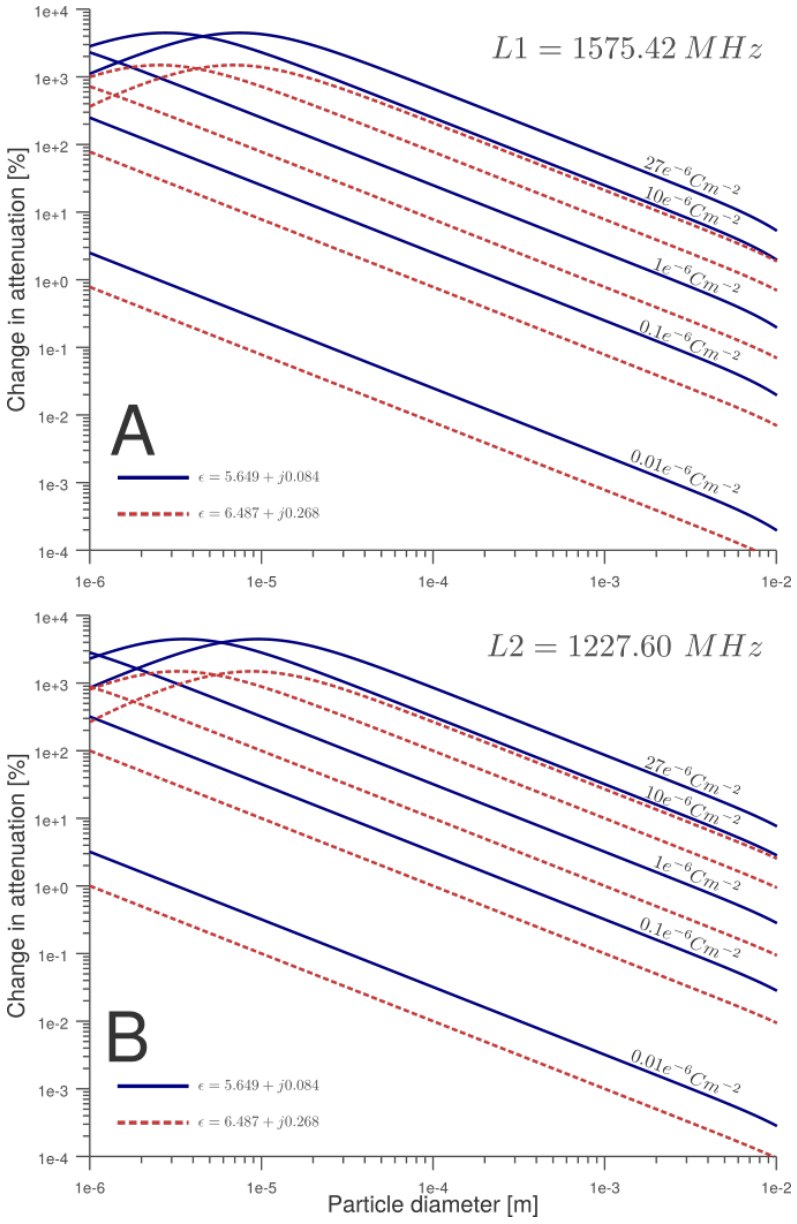

Figure 2.4: Change in attenuation (in percentage) as a function of charge density for both silicic (dashed red) and mafic (solid blue). A) For L1 = 1575.42 MHz. B) For L2 = 1227.60 MHz.

attenuate L-band signals by 1 dB at most. Yet, Larson et al. [2017] observed much larger attenuations during these eruptions. The modified Mie model presented above suggests that the ubiquitous electrification in ash-laden plumes may contribute significantly to signal degradation for L-band radiation. Due to absorption, Larson et al. [2017] indicate that grains with diameters ranging between 6 and 13 mm would produce path attenuations in the vicinity 0.014–0.109 dB km^{-1}. Because at those diameters, losses due to absorption equal those associated with scattering, the effective path attenuations would be 0.028–0.218 dB km^{-1}, resulting a maximum attenuation of 1 dB for a 5 km path-length. Observing Figures 2.2 and 2.3, such attenuation values would correspond to mass loadings of 10 -100 g m^{-3}. These elevated mass loadings imply that L-band signals are best suited to detect very dense plumes or signals that traverse the flow in close proximity to the vent. Such inference is consistent with observations at Etna and Redoubt [Larson et al., 2017]. If charging is included, however, the maximum path attenuation for the same mass loadings would increase to 0.3 - 3 dB km^{-1} for particles with diameters of several tens of microns. Across the same 5 km path length, the total attenuation would then range between 1.5 and 15 dB. While we do not discount the possibility that scattering from larger particles could explain additional losses (as suggested by Larson et al. [2017]), the calculation above suggests that if GPS is to be used as a tool to interrogate volcanic plumes, charge on particles must be taken into account.

2.4 Conclusion

In this work, we have applied a modified Mie model accounting for charge on particle surfaces to electrified volcanic plumes. Our results show that L-band radiation should be influenced by charged grains if these carry charge densities higher than 10^{-7} Cm^{-2} and they have sizes of several tens of microns. Additionally, we find that more mafic compositions attenuate centimeter-wave radiation more efficiently than more silica rich magmas. Furthermore, we have shown that the decreasing signal-to-noise ratio of GPS signals (in the

L-band) observed during the eruptions of Redoubt and Etna could be explained by electrification processes in the their ash-laden flows. Given that both of these volcanoes often produce volcanic lightning, particles in their plumes likely have charge densities of sufficient magnitude to produce measurable changes in the L-band signals. Future laboratory and experimental campaigns will validate our model.

CHAPTER 3
INDIRECT DETECTION OF ELECTROSTATIC INTERACTIONS BETWEEN MIRCON-SIZED PARTICLES IN A GRANULAR FLOW USING MILLIMETER-WAVES

This chapter is currently being formated for submission to the Journal of Electrostatics as Méndez Harper, J., Akins, A., Steffes, P., and Dufek, J. *Indirect detection of electrostatic interactions between particles in a granular flow using millimeter-waves*

3.1 Introduction

Granular flows, both natural and man-made, are often electrically charged [Baddeley, 1860; Cimarelli et al., 2016; Farrell et al., 2015; Gilbert et al., 1991; Hatakeyama, 1947; A. K. Kamra, 1972; A. Kamra, 1972; Thomas et al., 2007], producing anomalous electric and magnetic fields [Hatakeyama, 1947; Hatakeyama et al., 1951; Miura et al., 1996], large-scale discharges [Cimarelli et al., 2016; McNutt et al., 2010; Thomas et al., 2009], and, in some cases, changes to the dynamics of the granular system itself [Genareau et al., 2015; James et al., 2002]. Proposed charging mechanisms include triboelectric charging [Cimarelli et al., 2014; Méndez Harper et al., 2016], fractoelectrification [James et al., 2000; Méndez Harper et al., 2015], induction charging [Pahtz et al., 2010], electrification resulting from the decay of naturally-occurring radioactive isotopes in sand and ash grains [Aplin et al., 2014], and charging related to superficial layers of water [Arason et al., 2011; Gu et al., 2013; Xie et al., 2016]. Because electrification produces signals that can be detected from afar, characterizing the relationship between the flow dynamics and charging may catalyze the development of novel remote sensing techniques to monitor large-scale, natural granular flows. Such objective has received sizable attention in the context of large volcanic eruptions that can generate either large plumes which present hazards to avia-

tion or devastating pyroclastic density currents that endanger local populations [Arason et al., 2011; James et al., 1998; Méndez Harper et al., 2016]. However, understanding the links between flow properties and electrostatic processes has also important applications in industrial sectors, where charging of grains can lead to poor mixing of substances, flow disruption through pipes, and, in the work case, deadly dust explosions [Forward et al., 2009a; Hendrickson, 2006; Lacks, 2012; Lacks et al., 2007, 2011]. While numerous studies have described ways to characterize charging in granular flows using passive sensors (such as electric field mills and capacitive probes), a number of recent efforts have presented methodologies to actively interrogate substances with excess surface charge using electromagnetic radiation [Bohren et al., 1977; Chen et al., 2015; Gopalsami et al., 2009; Heifetz et al., 2010; Heinisch et al., 2012; Klačka et al., 2007; Kocifaj et al., 2015; Wang et al., 2013]. In essence, these approaches are founded on the idea that clouds of charged grains extinguish radiation differently than electrically-neutral collections of particles. Active methods may benefit from improved sensitivity with distance from the flow, better directional resolution, and require fewer sensors characterize volumetrically-large flows [Kocifaj et al., 2015]. Despite the promise of employing light, from microwave to optical wavelengths, to remotely study flows of electrified particles, only a few investigators, very recently, have explored the viability of such techniques experimentally or in the field. Using a simple one-particle system, Gopalsami et al. [2009] showed that the charge on a single cylindrical dielectric object could be detected using millimeter waves. Subsequently, Heifetz et al. [2010] used a similar setup to describe how charged water aerosols more effectively extinguished millimeter waves than their neutral counterparts. These researchers concluded that a charged particle can be treated as a composite grain with effective dielectric constant incorporating the volume dielectric function of the neutral sphere and a surface dielectric function arising from the motion of the surface charge in response to the exciting electric field. More recently, [Thiessen et al., 2014] studied the infrared extinction of charged dielectric core-coat particles, showing that such particles could be tailored

to be used as charge-sensitive markers in dusty plasmas. In this work, we experimentally investigate the interaction of millimeter waves (MMW) propagating through flows of micron-sized charged and neutral silicate particles. We show, that while the charge on particles cannot be directly assessed using MMW (in accordance with the modified Mie model for charged particles), such measurement techniques can detect changes in the dynamics of the flow resulting from electrostatic interactions between grains. Furthermore, we show that whether or not these changes can be resolved depends importantly in the shape of the particles. Particularly, we were able to detect electrostatic processes in flows composed of spherical particles. Our work reinforces the premise that MMW may serve as appropriate tools to study a diverse set of charged particle systems in man-made contexts as well as some natural ones.

3.2 Methods

To explore effect of electrification on the propagation of millimeter-waves through a granular flow, we constructed the apparatus shown in Figure 3.1 A and B. The device is functionally similar to the high-sensitivity millimeter-wavelength system used previously by Devaraj et al. [2011a] for measuring the opacity of gaseous sulfur dioxide under Venus conditions. The simulator comprises glass pressure chamber capable of sustaining pressures between 0 and 3 bars and temperatures up to 400 K. The glass chamber is T-shaped with the three apertures closed-off with aluminum end-caps. The lower end-cap supports a fluidizing cup capable of holding approximately 413 cm^3 of a granular material. A 300-μm hole in the base of the cup allows the passage of a gas stream, producing a spouted bed with a nominal fountain height of 8-9 cm. The lateral end-caps sustain a pair of confocal, gold-plated curved mirrors (one each) separated by a distance of 14.2 cm. This arrangement forms a Fabry-Perot resonator (FPR), an open electromagnetic cavity which exhibits periodic, salient peaks in field strength (resonances) when the distance between the mirrors is equal to an integer multiple of the half wavelength of the radiation coupled to the cavity.

Devices like this one are differentiated from other dielectric metrological tools by being a multi-path system. In other words, the operation of the FPR can be analyzed in terms of standing-waves between the curved reflectors [Clarke et al., 1982]. As such, the radiation path-length through the material-under-test (MUT; in this case the particle fountain) can be on the order of several hundred meters, giving an FPR exceptional sensitivity to changes in the MUT. FPRs have been used in a variety of applications including magnetic resonance studies, dielectric spectroscopy, atmospheric measurements, and planetary science [Bellotti et al., 2015; Devaraj et al., 2011b]. The setup described here has been tuned to use in the W-band region of the electromagnetic spectrum (75-110 GHz). A synthesized swept signal generator (HP 83650B) is employed to produce a signal in the 12.5-18.3 GHz range. This signal is then fed to a times-six active multiplier chain (AMC). The active multiplier outputs a W-band signals which is delivered to the FPR input port via WR-10 waveguides. At the output port of the FPR, the signal is fed via waveguide to a QuinStar Technology QMH series harmonic mixer. The local oscillator (LO) and the intermediate frequency (IF) are connected using an external diplexer. The harmonic mixer is locked to the 18th harmonic of a HP 8564E spectrum analyzer LO. The signal generator was operated in external mixer mode. The data acquisition system consists of a computer connected to the spectrum analyzer (HP 8564E), swept signal generator (HP 83650B), and a signal generator (HP 83712B) via a general purpose interface bus (GPIB). The instruments are controlled through a Matlab script.

Prior to conducting an experiment, the chamber is evacuated to a pressure less than 100 Pa to minimize the effects of water. The chamber is then filled with nitrogen to a pressure of 0.1 MPa and allowed to equilibrate overnight. As mentioned above, fountaining is accomplished by passing a narrow nitrogen stream through the bottom of the particle bed. To keep the pressure in the vessel constant throughout an experiments, a mass flow controller vents gas from the chamber to counteract the mass added in the fountaining process. To generate the fountain itself we utilize two granular materials: glass beads and volcanic

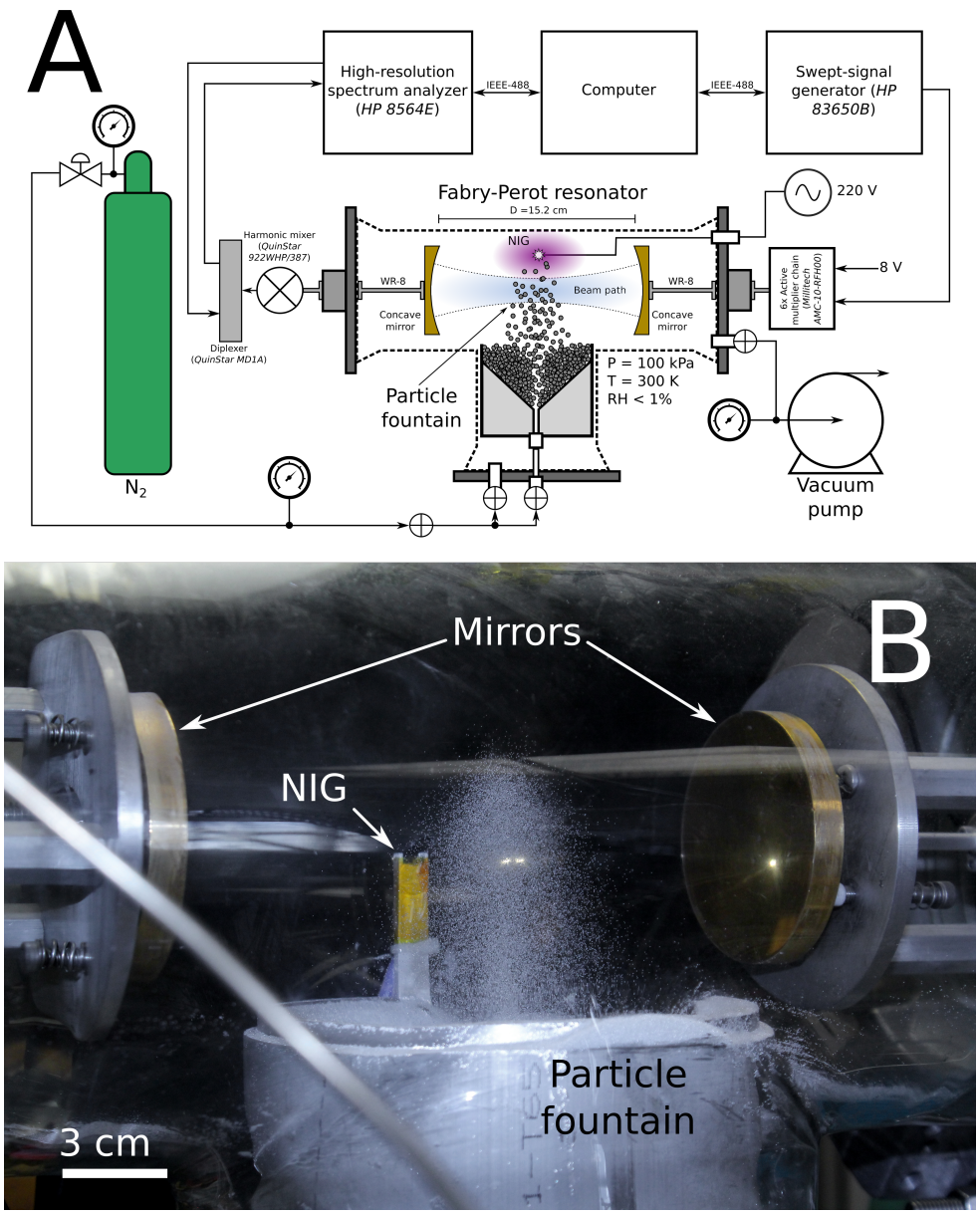

Figure 3.1: Schematic (A) and photograph (B) of the Fabry-Perot resonator used in this work

ash (from Mount St. Helens), both with a nominal grain size distribution between 125 and 250 microns (See Figure 3.2 A and B). We selected these materials because they have similar chemical compositions (both silicates), but have vastly different shapes. Whereas glass beads are fairly spherical, volcanic ash particles are highly angular. This allows us to explore the manner in which millimeter waves interact with charged particles of different morphologies. During an experiment, the dynamics of the fountain were monitored by illuminating the flow with a laser sheet and taking a photograph every second. When fluidized, particles charge naturally through triboelectrification–that is, via contact and frictional charging–with small particles concentrating negative charge, while larger grains, on average, gain positive charge. However, because charge is exchanged primarily between constituent particles in the experimental setup, the fountain as a whole remains nominally neutral. Thus, to bias the fountain with a known amount of charge we exposed the flow to an ion cloud produced by a negative ion generator (NIG) placed 75 mm away from the fountain's centerline. The NIG consists of a high-voltage supply (20 kV) wired to a bundle of sharp carbon needles which serve to breakdown the surrounding atmosphere. Ions attach to lofted particles, giving them a net negative charge. At the fountain, the ion production rate is approximately 10×10^6 ions/cm^3/s.

In this work, we focus on two W-band resonances: one near the lower end of the band at 82.8 GHz and one near the higher end at 104.3 Ghz. In a purely gaseous environment (nitrogen gas), resonances follow Lorentzian distributions (See Figure 3.3). While our photographic series shows that the fountaining reaches steady-state after a few seconds after the initiation of fluidization, small scale oscillations in the plume remain present throughout. Such variations introduce significant noise in the data. Thus, line-shapes associated with the particle fountain (displayed below) were obtained by averaging 10 measurements.

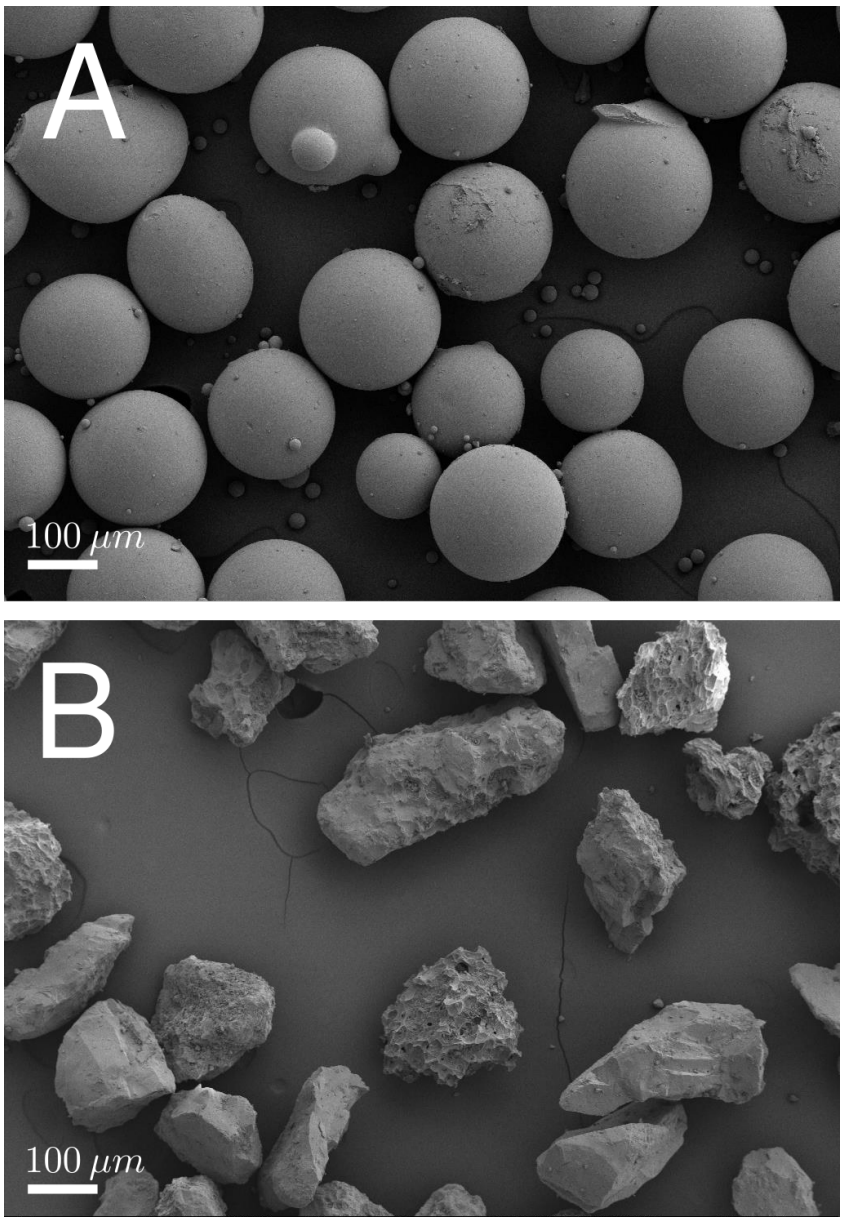

Figure 3.2: Particles used in this study. A) Glass spheres and B) volcanic ash from Mount Saint Helens. Both granular materials have nominal grain size distributions between 125 and 250 microns.

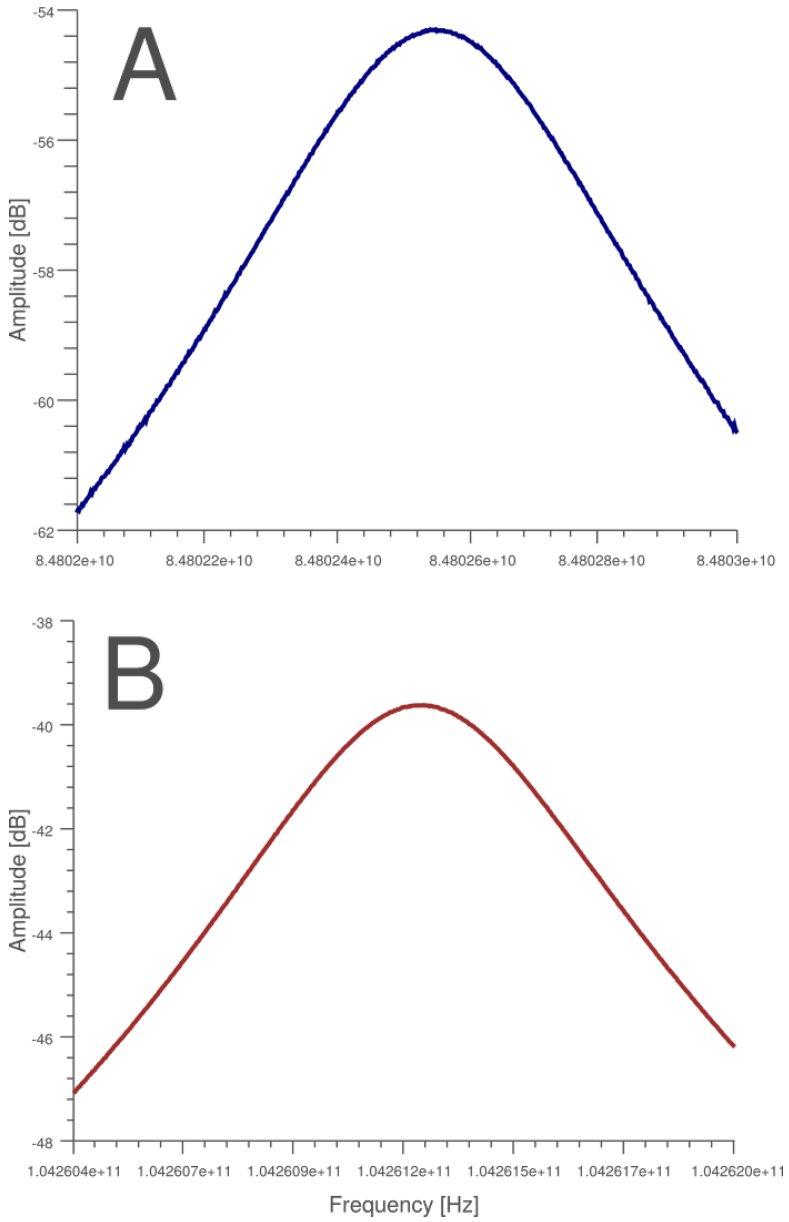

Figure 3.3: W-band resonances observed in a pure N_2 atmosphere. A) Near 82.8 GHz. B) Near 104.3 GHz.

3.3 Results and discussion

The quality factor Q_{factor} of a resonant mode of a resonator can be used to measure the absorption of a gas or gas mixture. The quality factor for a particular resonance is given by:

$$Q_{factor} = \frac{2\pi f_0 E_s}{< P >} \tag{3.1}$$

where f_0 is the resonant frequency, E_s is the stored energy in the resonator, and $< P >$ is the average power loss. Alternatively, the quality factor of a resonance can be measured directly from the resonant frequency by dividing it by its half-power bandwidth, $HPBW$.

$$Q_{factor} = \frac{f_0}{HPBW} \tag{3.2}$$

Knowing the quality factor for a lossy media, Q_m, one can compute the attenuation, α, as:

$$\alpha = \frac{1}{Q_m}\pi\lambda \tag{3.3}$$

Resonances for a pure nitrogen environment (no fountain) are rendered in Figure 3.3. These resonances are characterized by quality factors of 14.6×10^3 and 20.7×10^3 for the resonance at 82.4 GHz and 104.3 GHz, respectively. Introducing the particle fountain (composed either of glass beads or ash grains) causes a downward shift in frequency and a decrease in quality factor (5.14×10^3 for the resonance near 82.4 GHz and 5.17×10^3 for the resonance downshifted from 104.3 GHz), indicating that the two granular materials are both refractive and lossy (Figures 3.4 and 3.5). Surprisingly, the addition of charge to the system (by turning on the NIG) results in vastly different behaviors between the system composed of glass beads and that of volcanic ash. For the fountain of glass beads, we observe that the there is a upward shift in the resonant center frequencies (See Figure 3.4), with corresponding changes in Q factors to 5.16×10^3 and 6.46×10^3 for the resonances near 82.4 and 104.3 GHz, respectively. Yet, there is little or no change in the

millimeter wave response for the fountain of volcanic ash (See Figure 3.5). To disentangle the underlying cause of these behaviors, we first investigate whether they result from the interaction between the MMW and the surface charge. The effects of surface charge on the propagation of electromagnetic radiation through a fluidized granular media has been explored by Bohren et al. [1977], Klačka et al. [2007], Heifetz et al. [2010], Klacka et al. [2010], and Kocifaj et al. [2015]. These authors have shown that under certain conditions surface charge can have important consequences for scattering and absorption. From a classical electrodynamic standpoint, the charge on a spherical particle can be analyzed using conventional Mie theory with modifications to the equation of continuity of tangential magnetic fields at the boundary of the sphere:

$$\mathbf{n}\times(\mathbf{H}_2 - \mathbf{H}_1) = \mathbf{K} \tag{3.4}$$

where $\mathbf{K}$ is the surface current density which can be expressed in terms of a phenomenological surface conductivity, σ_s, and the tangential electric field, $\mathbf{E}_{1,T}$:final

$$\mathbf{K} = \sigma_s \mathbf{E}_{1,T}. \tag{3.5}$$

Alternatively, 3.5 can be rendered as a function of the surface charge density, η, and the velocity of the surface charge carriers, $\mathbf{u}$:

$$\mathbf{K} = \eta \mathbf{u}. \tag{3.6}$$

Thus, as shown by Bohren et al. [1977], the surface charge can be included into the Mie model through an effective surface dielectric function:

$$\epsilon_s = -\omega_s^2/(\omega^2 + j\omega\gamma) \tag{3.7}$$

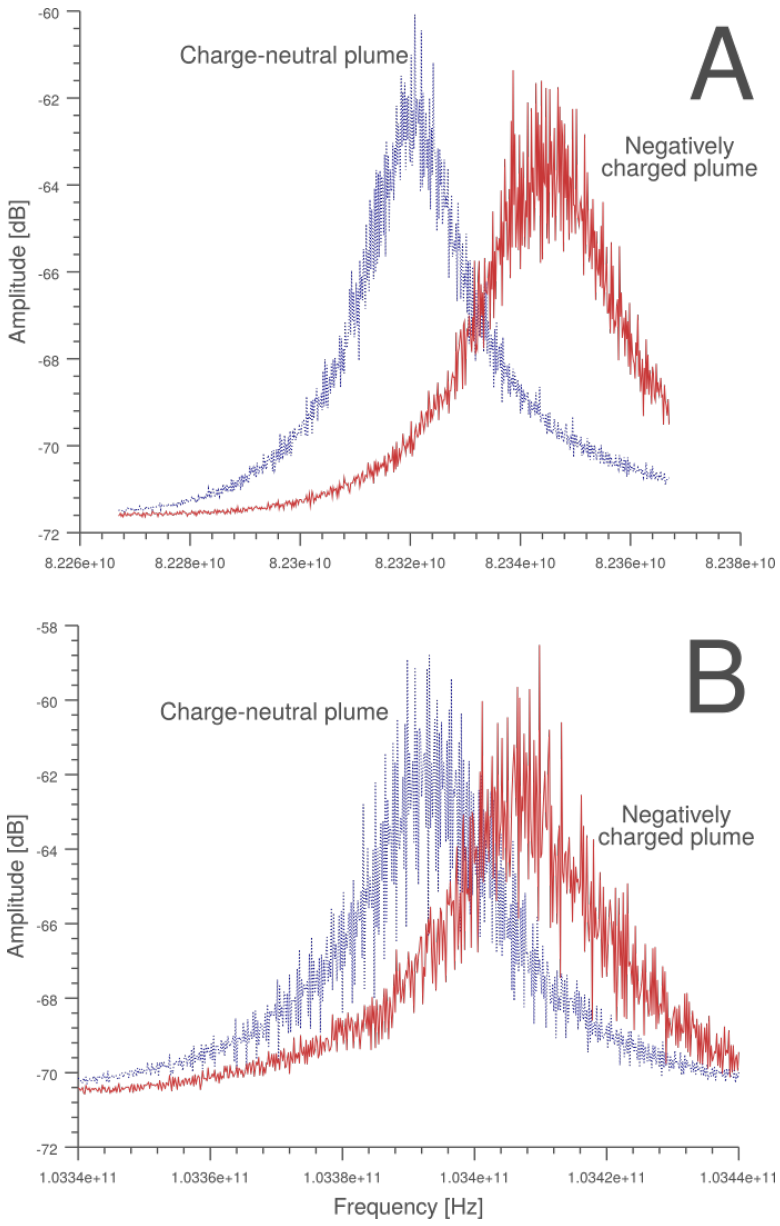

Figure 3.4: W-band resonances observed in the experiments with glass beads for a charged fountain (solid red) and uncharged fountain (dashed blue). A) Near 82.3 GHz. B) Near 103.4 GHz.

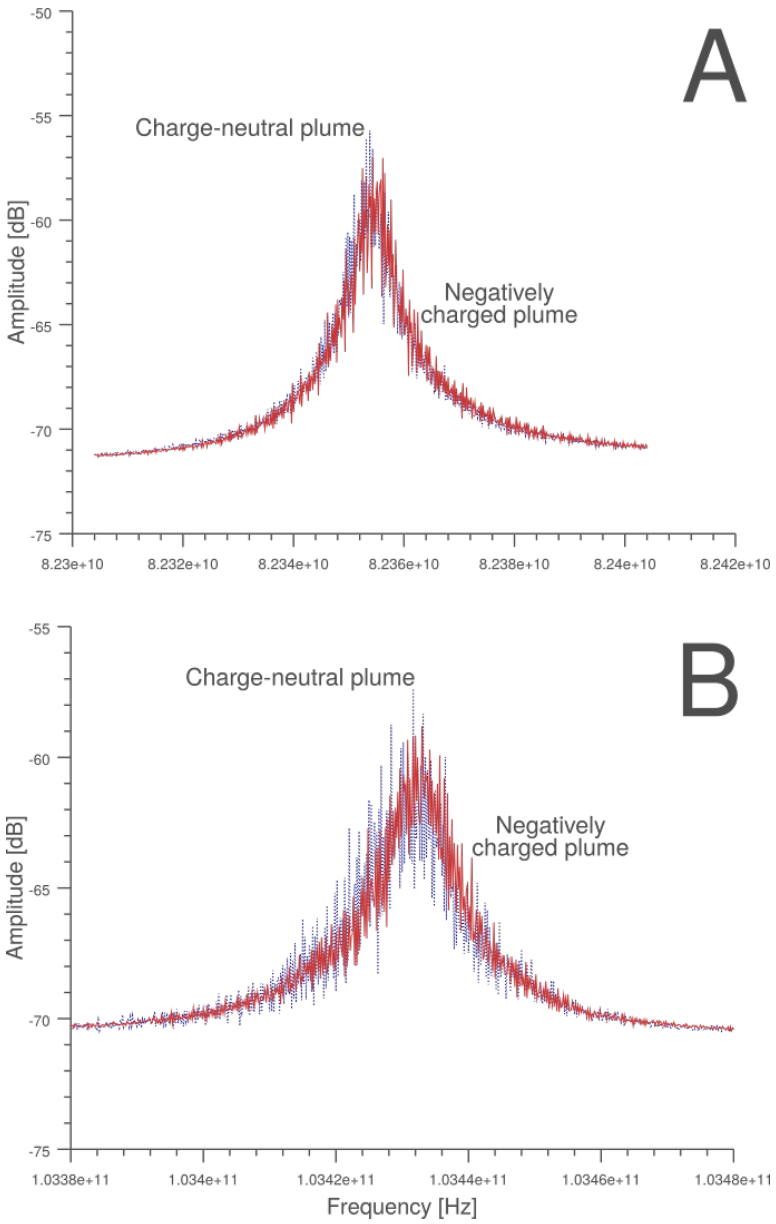

Figure 3.5: W-band resonances observed in the experiments with volcanic ash for a charged fountain (solid red) and uncharged fountain (dashed blue). A) Near 82.3 GHz. B) Near 103.4 GHz.

where the surface plasma frequency can be defined as:

$$\omega_s^2 = Ne^2/(2\pi Rfinal^3 m_e \epsilon_0). \tag{3.8}$$

In Equation 3.8, N is the total number of charge carriers, e is the elementary charge, m_e is the electron mass, R is the particle radius, and ϵ_0 is the permittivity of free space. γ (Equation 3.7) is a damping constant equal to $k_B T/\hbar$, where k_B is the Boltzmann constant, $\hbar$ is the reduced Plank constant, and T is temperature in Kelvin. A full mathematical solution to the modified Mie model is described in Klačka et al. [2007], Klacka et al. [2010], and Kocifaj et al. [2015]. Using this formulation, the effects of charge on the absorption, scattering, and total extinction efficiencies for millimeter waves are rendered in Figure 3.6 as a function of the size parameter (that is $x = 2R\pi/\lambda$). There, we have plotted the attenuation efficiencies for a charged grain relative to those of an uncharged particle. As can be seen, charging only impacts extinction when x becomes smaller than $\sim$ 0.01. As mentioned previously, we used particles with nominal diameters between 125-250 μm. Thus, for W-band signals, with wavelengths of 2.7 - 4 mm, our experimental system is characterized by size parameters ranging between 0.1 and 0.3. In other words, we find it unlikely that the surface charge would have any direct effect on the propagation of millimeter waves. An alternative explanation can be found in the photographic series taken during the experiments. When the NIG is active, the fountain of glass beads expands geometrically in both the vertical and horizontal directions (Figure 3.7). Furthermore, we see that the morphology of the particle bed is impacted by the charging. Indeed, charged glass particles are attracted to the grounded fluidizing cup, forming an electrostatic crust on its surface. This, "sheeting" (Figure 3.8) does not occur when the NIG is inactive. Such effects can be explained by the manner in which grains are electrified in our experiments. Charged with the ionizing source, particles collect unipolar charge on their surfaces–in this case negative. Thus, the expansion seen in the fountain is likely the result of mutual repulsion between grains. Such

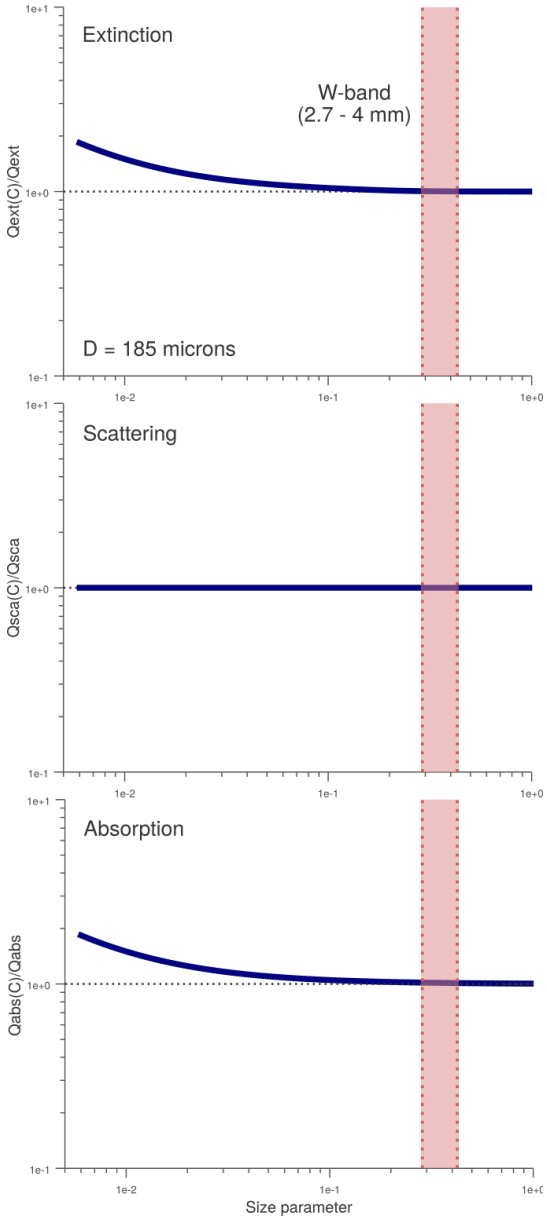

Figure 3.6: Ratio of efficiency factors (A) Extinction, B) Absorption, and C) Scattering) for charged and non-charged silicate particles as function of size parameter. Shaded region indicates the operating conditions for experiments. Note that charging on sub-millimeter particles unlikely influences the propagation of millimeter waves.

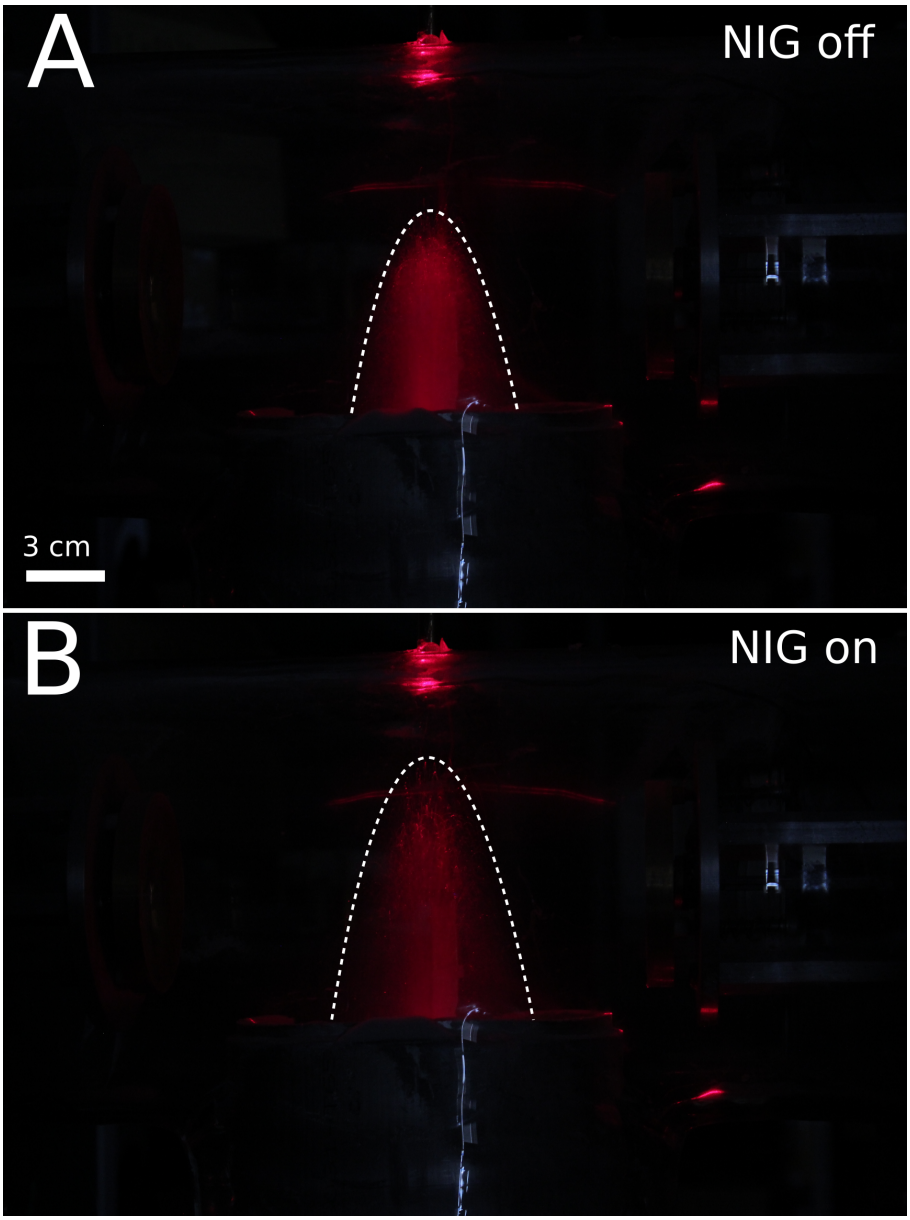

Figure 3.7: Morphology of the glass bead fountain A) with the NIG inactive and B) with the NIG active. Note the expansion of the fountain when particles are charged.

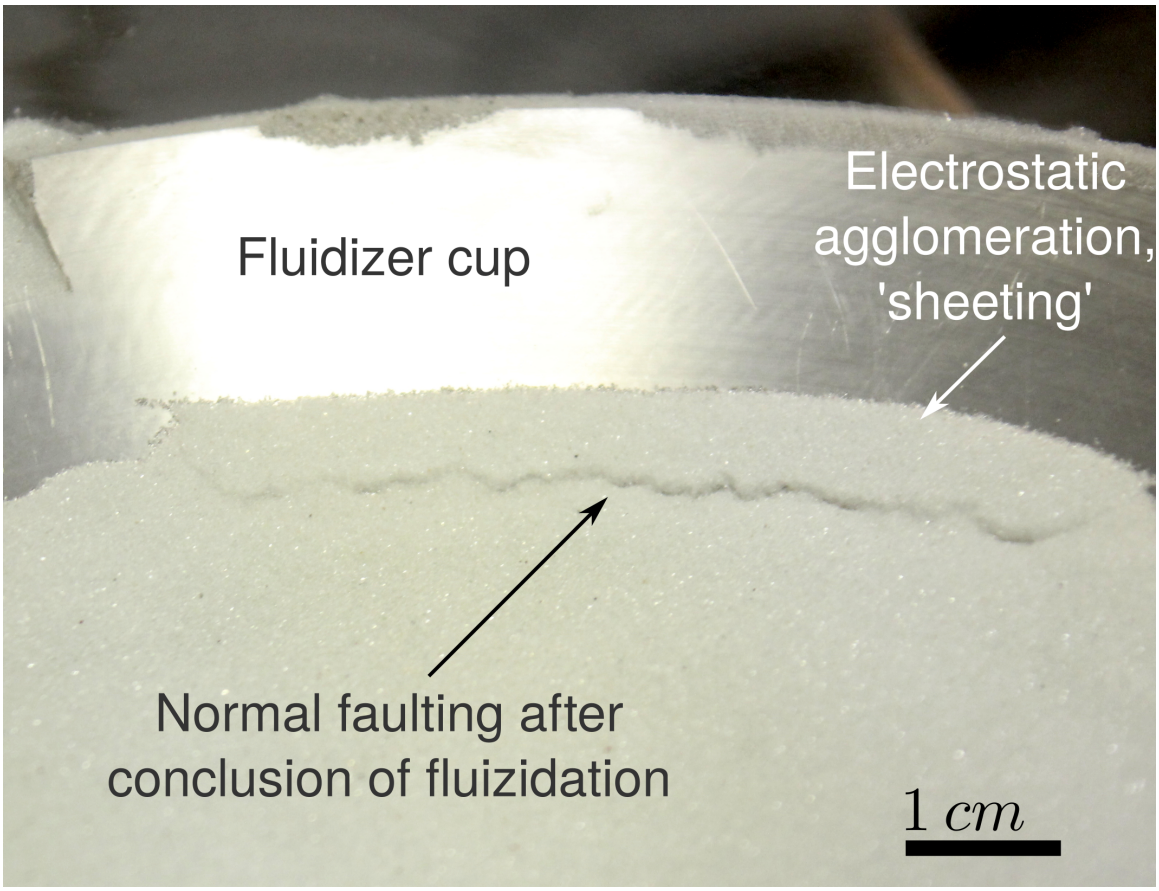

Figure 3.8: Agglomerates or aggregates observed in experiments with charged glass beads. Such phenomenon is often referred to as “sheeting.”

behavior stands in contrast to that observed when particles self-charge triboelectrically, during which the granular material charges bipolarly, increasing cohesive forces between individual grains, producing a more collimated fountain. As the fountain expands resulting from electrostatic repulsion, the mass loading–i.e. the number of particles per unit volume–decreases, making the flow less opaque and refractive to millimeter waves. A significantly different behavior is observed in the flow of ash grains. As rendered in Figure 3.9, the NIG has little or no consequence on the dynamics of the spouted bed. Indeed, we did not observe an analogous expansion of the fountain or sheeting on the walls of the fluidizing cup. Correspondingly, the absence of hydrodynamical variations in the fountain resulted in insignificant changes in the the propagation behavior of the imposed millimeter-waves. Mizuno et al. [1985] conducted experiments with non-spherical particles to show that grains with sharp edges tend to gain saturation charges that are smaller than those of their spherical counterparts (by as much as a factor of 2). This effect is explained by the fact the highly angular grains lose charge through corona discharge at edges where the electric field may exceed the breakdown field. While their analysis focused on highly conductive grains, this effect would still be observed in ash particles which are only moderately insulating. Thus, we hypothesis that, by virtue of their angular shapes (Figure 3.2), ash particles are able to retain charge less effectively than the spherical glass beads. Furthermore, in a fluidized bed, where particles undergo copious particle-particle collisions, charge depletion on irregular particles may be enhanced through contact *de-electrification*. Indeed, Soh et al. [2012] recently demonstrated that the interaction between particles charged to the same polarity leads to charge loss as the electric field at the point of contact between two grains exceeds the breakdown limit. We note that such phenomenon would operate in both the glass and ash fountains. However, we infer that the effect would be enhanced in the ash fountain because the electric fields at the points where ash grains come into contact (i.e. sharp tips) are higher than at the contact points between spherical particles (smoother surfaces). In essence, the lower charge-to-mass ratio of ash particles would reduce the importance of

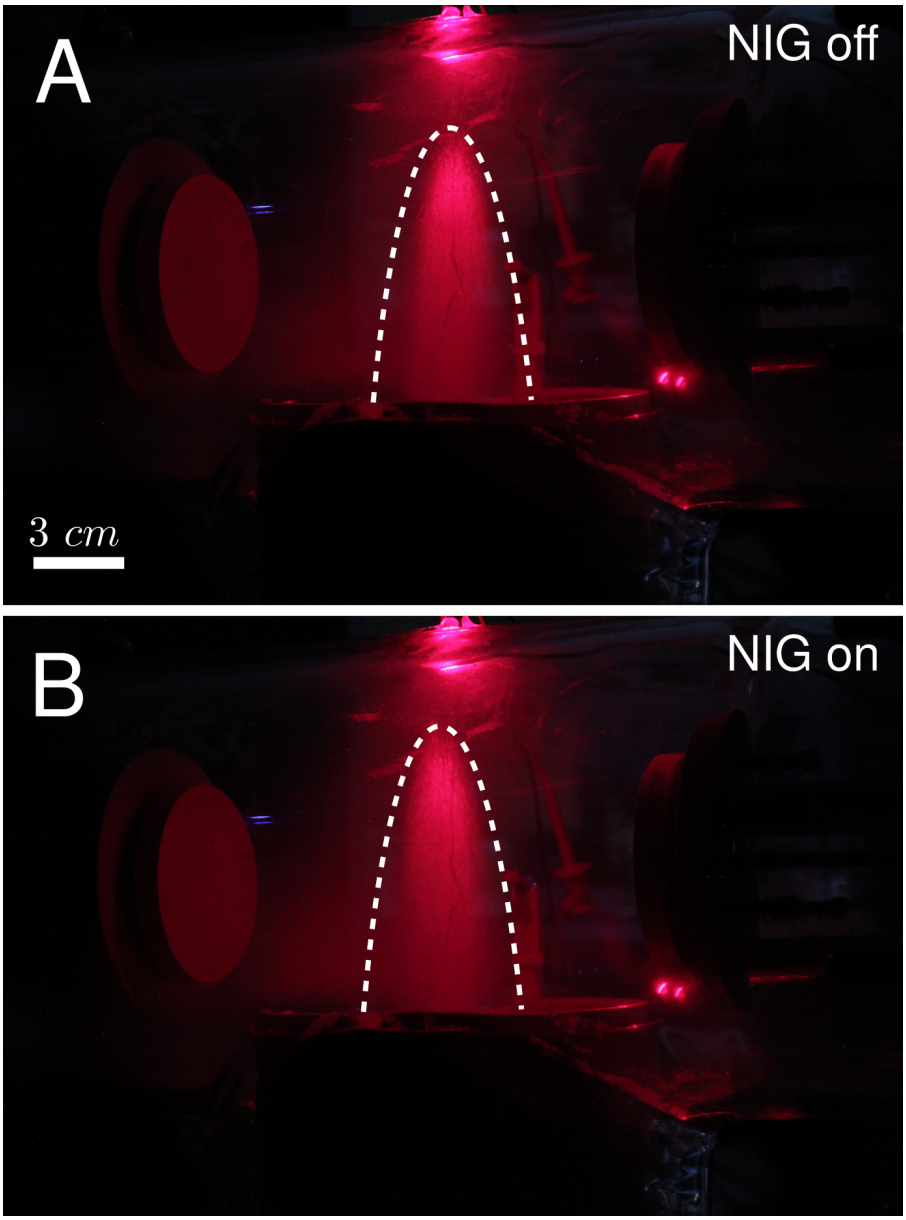

Figure 3.9: Morphology of the ash fountain A) with the NIG inactive and B) with the NIG active. Note the little change between the uncharged and charged cases.

electrostatic forces between particles as compared to inertial ones, resulting in a charged fountain whose dynamics would not vary significantly from the electrically-neutral one.

3.4 Conclusion

Here, we have presented the results of a set of experiments designed to characterize the interaction of millimeter waves with micron-sized unipolarly charged dielectric particles. Our work demonstrates that while the size parameters charactering the system are too large for surface charge to be of direct consequence to the propagation of W-band radiation (as described by the modified Mie models of Bohren et al. [1977] and Klačka et al. [2007]), we were able to detect changes in the dynamics of the charged granular flow resulting from electrostatic interactions between the grains. Using particles with considerably different morphologies (glass beads and volcanic ash), we found that electrostatic forces importantly modified the hydrodynamics of a spouted bed spherical grains, but had little bearing on a similar flow of angular grains. We attribute the lack of electrostatic effects in the flow of ash particles their angular surfaces which increase the probability of corona discharge at angular tips. Given that most particles in nature are non-spherical, the work present here may find limited applications in the geophysical contexts. However, our experiments show that millimeter waves should be investigated further as potential tools to characterize and monitor industrial systems dealing with spherical particles.

CHAPTER 4
CONTINUING WORK: THE EFFECTS OF CHARGED PARTICLES ON THE PROPAGATION OF CENTIMETER-WAVE RADIATION

In this chapter, we describe continuing work relating to the characterization of charged granular flows with electromagnetic radiation.

4.1 Characterizing charged particles with L-band wavelengths

As we discussed in Chapters 2 and 3, modified versions of Mie's classical theory suggest that charge trapped on the surfaces of particles can effectively attenuate electromagnetic radiation if the wavelength is approximately 100 times larger than the diameters of the illuminated particles [Bohren et al., 1977; Heifetz et al., 2010; Klačka et al., 2007; Klacka et al., 2010; Kocifaj et al., 2015]. In particular, we are interested validating the numerical model presented in Chapter 2–the hypothesis that charged volcanic plumes can be assessed using readily available GPS signals (L-band). To further investigate the dielectric properties of charged granular flows, we have designed the "cut-off" coaxial probe rendered in Figure 4.1. In essence, the system consists of a coaxial waveguide which transitions to a circular waveguide [Kaatze, 2010]. To ensure correct operation, this last portion of the system must be operated well below the cut-off frequency of its TM_{01} mode when filled with the material under test. The microwave characteristics of the material with the cell is obtained by measuring the reflected power from the sample. Such probes are extremely versatile, with the ability to be operated over a frequency range spanning from 1 MHz to approximately 50 GHz [Kaatze, 2010]. These sensors find applications in the characterization of agricultural products, biological and chemical substances, and soil samples [Alanen et al., 1999; Lazebnik et al., 2007; Schimmer et al., 2007; Sheen et al., 1999].

In addition to being a measurement device, the cell shown in Figures 4.1 and 4.2 serves

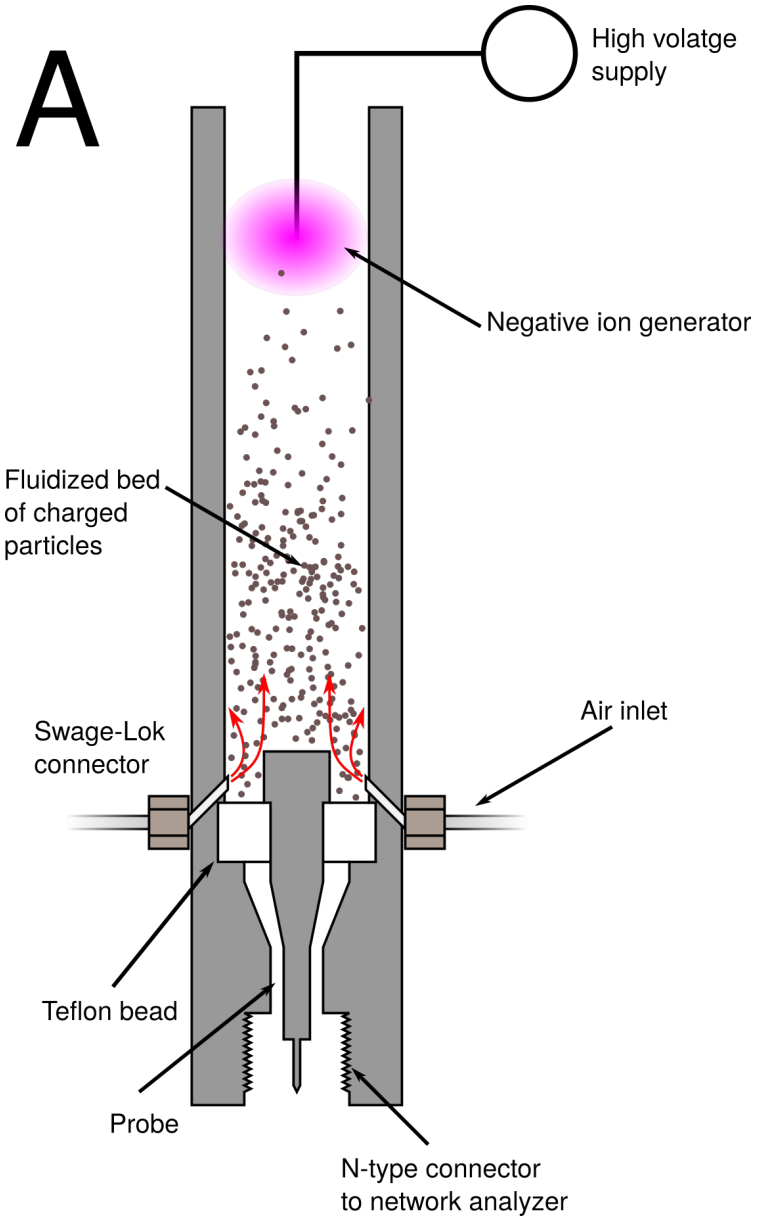

Figure 4.1: Schematic of coaxial probe to measure the effective dielectric constant of charged ash grains with L-band radiation. Not to scale.

as a fluidization chamber. Prior to making a measurement a certain amount of granulated material is placed within the cell. The measurement volume is closed off from the measurement electronics (in this case a vector network analyzer) by a fitted PTFE bead. Just above the bead, the sensor has apertures through which a gas can be injected to fluidize the granular material. Once mobilized the grains are charged with a negative ion generator position near the top of the cell.

The device has been designed to have an impedance of 50 ohms and a cut-off frequency of 6 GHz. Like the material employed in the experiments described in Chapter 3, the particles in this effort have nominal grain size distributions between 125 and 250 microns. Excited with L-band radiation (with wavelengths around 20 cm), the system will be characterized by size parameters in the range of 0.005 - 0.01. Under such conditions we should be able to detect changes to the effective dielectric function modulated by surface charge on grains. The coaxial probe is shown photographically in the Figure 4.2.

Figure 4.2: Photograph of manufactured coaxial probe to measure the effective dielectric constant of charged ash grains. L-band radiation.

CHAPTER 5
CONCLUSION

In the present work, we explored, both numerically and experimentally, the manner in which charging affects the propagation of electromagnetic waves through charged volcanic plumes. Using a modified Mie model, we determined that GPS (or other L-band radiation) could be used to extract information about the level of electrification in volcanic plumes. The results of our model were compared to the anomalous GPS signals obtained by Larson, 2013 and Larson et al., 2017 and we infer that the behaviors of such signals could be accounted for by charging the volcanic systems. While the work regarding the propagation of L-band radiation through charged media was only treated in the present effort numerically, we intend to continue our investigations both in laboratory settings as well as in the field. One potential field site for such a study is the Tonaltepetl volcano in the western Mexican states of Xalixco and Colliman. A small stratovolcano, Tonaltepetl erupts several times a day and often produces brilliant displays of lightning (i.e it generates highly electrified granular flow). The second stage of this project involved experiments to determine the interaction between W-band light (millimeter waves) and charged particles of several hundreds of microns. Only recently has W-band radiation been considered (in a numerical fashion) as a potential tool for monitoring volcanoes (See Bryan et al., 2017), but, again, the effects of charging were not explored. Our experimental setup consists of a spouted bed to disperse grains in air (similar to that described in Méndez Harper et al., 2016). The resulting fountain is placed in the beam path of a Fabry-Perot resonator (FPR). This endeavor made use of heritage technology developed at Georgia Tech in the Planetary Atmosphere's Lab [Devaraj et al., 2011a]. Such devices have been used to characterize the simulated Venusian and Jovian atmospheres (e.g. [Bellotti et al., 2015]). While we found that millimeter waves cannot directly detect charge on particles with diameters of several hundreds

of microns, we showed that electrostatic interactions between charged particles could be resolved changing dynamics altered the number of particles in the sensing volume of the FPR. We also found that electrostatic effects were most pronounced when grains were spherical. While the results of this part of the work may not find application in volcanology (in which particles are highly angular), they may be of interest to those in industrial sectors that deal with regularly-shaped grains.

BIBLIOGRAPHY

Adams, Rob J et al. (1996). "Measurements of the complex dielectric constant of volcanic ash from 4 to 19 GHz". In: *Journal of Geophysical Research: Solid Earth* 101.B4, pp. 8175–8185.

Aizawa, Koki et al. (2016). "Physical properties of volcanic lightning: Constraints from magnetotelluric and video observations at Sakurajima volcano, Japan". In: *Earth and Planetary Science Letters* 444, pp. 45–55.

Alanen, Esko, Tapani Lahtinen, and Jouni Nuutinen (1999). "Penetration of electromagnetic fields of an open-ended coaxial probe between 1 MHz and 1 GHz in dielectric skin measurements". In: *Physics in medicine and biology* 44.7, N169.

Aplin, Karen L., Isobel M. P. Houghton, and Keri A. Nicoll (2014). "Electrical charging of ash in Icelandic volcanic plumes". In: *arXiv:1404.6905 [physics]*. arXiv: 1404.6905.

Apodaca, Mario M et al. (2010). "Contact electrification between identical materials". In: *Angewandte Chemie* 122.5, pp. 958–961.

Aranzulla, Massimo et al. (2013). "Volcanic ash detection by GPS signal". In: *GPS solutions* 17.4, pp. 485–497.

Arason, Pordur, Alec J. Bennett, and Laura E. Burgin (2011). "Charge mechanism of volcanic lightning revealed during the 2010 eruption of Eyjafjallajokull". In: *Journal of Geophysical Research: Solid Earth* 116.B9, B00C03.

Baddeley, PFH (1860). *Whirlwinds and dust-storms of India*. Bell & Daldy.

Behnke, Sonja A. and Eric C. Bruning (2015). "Changes to the turbulent kinematics of a volcanic plume inferred from lightning data". In: *Geophysical Research Letters* 42.10, 2015GL064199.

Behnke, Sonja A. et al. (2012). "Spectacular lightning revealed in 2009 Mount Redoubt eruption". In: *Eos, Transactions American Geophysical Union* 93.20, pp. 193–194.

Behnke, Sonja A. et al. (2013). "Observations of volcanic lightning during the 2009 eruption of Redoubt Volcano". In: *Journal of Volcanology and Geothermal Research*. The 2009 Eruption of Redoubt Volcano, Alaska 259, pp. 214–234.

Bellotti, Amadeo and Paul G Steffes (2015). "The millimeter-wavelength sulfur dioxide absorption spectra measured under simulated Venus conditions". In: *Icarus* 254, pp. 24–33.

Bohren, Craig F and Donald R Huffman (2008). *Absorption and scattering of light by small particles*. John Wiley & Sons.

Bohren, Craig F and Arlon J Hunt (1977). "Scattering of electromagnetic waves by a charged sphere". In: *Canadian Journal of Physics* 55.21, pp. 1930–1935.

Bryan, Sean et al. (2017). "Measuring Water Vapor and Ash in Volcanic Eruptions With a Millimeter-Wave Radar/Imager". In: *IEEE Transactions on Geoscience and Remote Sensing* 55.6, pp. 3177–3185.

Chen, YY et al. (2015). "Scattering of terahertz wave by charged spherical particles". In: *Indian Journal of Physics* 89.3, pp. 299–305.

Cimarelli, C. et al. (2014). "Experimental generation of volcanic lightning". In: *Geology* 42.1, pp. 79–82.

Cimarelli, C. et al. (2016). "Multiparametric observation of volcanic lightning: Sakurajima Volcano, Japan". In: *Geophysical Research Letters* 43.9, 2015GL067445.

Clarke, RN and CB Rosenberg (1982). "Fabry-Perot and open resonators at microwave and millimetre wave frequencies, 2-300 GHz". In: *Journal of Physics E: Scientific Instruments* 15.1, p. 9.

Devaraj, Kiruthika and Paul G Steffes (2011a). "The Georgia Tech millimeter-wavelength measurement system and some applications to the study of planetary atmospheres". In: *Radio Science* 46.2.

Devaraj, Kiruthika, Paul G Steffes, and Bryan M Karpowicz (2011b). "Reconciling the centimeter-and millimeter-wavelength ammonia absorption spectra under jovian conditions: Extensive millimeter-wavelength measurements and a consistent model". In: *Icarus* 212.1, pp. 224–235.

Dou, XQ and L Xie (2017). "Electromagnetic wave attenuation due to the charged particles in dust&sand (DUSA) storms". In: *Journal of Quantitative Spectroscopy and Radiative Transfer* 196, pp. 169–175.

Eaton, Nicholas (1984). "Comet dust-applications of Mie scattering". In: *Vistas in Astronomy* 27, pp. 111–129.

Farrell, W. M. et al. (2015). "Is the electron avalanche process in a martian dust devil self-quenching?" In: *Icarus* 254, pp. 333–337.

Forward, Keith M., Daniel J. Lacks, and R. Mohan Sankaran (2009a). "Charge Segregation Depends on Particle Size in Triboelectrically Charged Granular Materials". In: *Physical Review Letters* 102.2, p. 028001.

— (2009b). "Particle-size dependent bipolar charging of Martian regolith simulant". In: *Geophysical Research Letters* 36.13, p. L13201.

Genareau, Kimberly et al. (2015). "Lightning-induced volcanic spherules". In: *Geology* 43.4, pp. 319–322.

Gilbert, J. S. et al. (1991). "Charge measurements on particle fallout from a volcanic plume". In: *Nature* 349.6310, pp. 598–600.

Gopalsami, Nachappa et al. (2009). "Millimeter wave detection of nuclear radiation: An alternative detection mechanism". In: *Review of scientific instruments* 80.8, p. 084702.

Gu, Zhaolin et al. (2013). "The role of water content in triboelectric charging of wind-blown sand". In: *Scientific Reports* 3, p. 1337.

Harrison, R. G. et al. (2010). "Self-charging of the Eyjafjallajokull volcanic ash plume". In: *Environmental Research Letters* 5.2, p. 024004.

Hatakeyama, H. (1947). "On the Variation of the Atmospheric Potential Gradient caused by the Cloud of Smoke of the Volcano Asama. (The Fourth Report.)" In: *Journal of the Meteorological Society of Japan. Ser. II* 25.1-3, pp. 39–39.

Hatakeyama, H. and K. Uchikawa (1951). "On the Disturbance of the Atmospheric Potential Gradient caused by the Eruption-smoke of the Volcano Aso". In: *Papers in Meteorology and Geophysics* 2.1, pp. 85–89.

Heifetz, Alexander et al. (2010). "Millimeter-wave scattering from neutral and charged water droplets". In: *Journal of Quantitative Spectroscopy and Radiative Transfer* 111.17, pp. 2550–2557.

Heinisch, Rafael L, Franz X Bronold, and Holger Fehske (2012). "Mie scattering by a charged dielectric particle". In: *Physical review letters* 109.24, p. 243903.

Hendrickson, Gregory (2006). "Electrostatics and gas phase fluidized bed polymerization reactor wall sheeting". In: *Chemical Engineering Science* 61.4, pp. 1041–1064.

Houghton, Isobel M. P., Karen L. Aplin, and Keri A. Nicoll (2013). "Triboelectric Charging of Volcanic Ash from the 2011 Gr\'{\i}msv\"otn Eruption". In: *Physical Review Letters* 111.11, p. 118501.

Houlié, Nicolas et al. (2005). "Sounding the plume of the 18 August 2000 eruption of Miyakejima volcano (Japan) using GPS". In: *Geophysical research letters* 32.5.

Hulst, Hendrik Christoffel (1957). *Light scattering by small particles*. Courier Corporation.

James, Mike, J. S. Gilbert, and S. J. Lane (2002). "Experimental investigation of volcanic particle aggregation in the absence of a liquid phase". In: *Journal of Geophysical Research: Solid Earth* 107.B9, p. 2191.

James, Mike, S. J. Lane, and J. S. Gilbert (2000). "Volcanic plume electrification: Experimental investigation of a fracture-charging mechanism". In: *Journal of Geophysical Research: Solid Earth* 105.B7, pp. 16641–16649.

James, Mike, SJ Lane, and JS Gilbert (1998). "SPECIAL: Volcanic plume monitoring using atmospheric electric potential gradients". In: *Journal of the Geological Society* 155.4, pp. 587–590.

Kaatze, Udo (2010). "Techniques for measuring the microwave dielectric properties of materials". In: *Metrologia* 47.2, S91.

Kamra, A. K. (1972). "Measurements of the electrical properties of dust storms". In: *Journal of Geophysical Research* 77.30, pp. 5856–5869.

Kamra, AK (1972). "Physical sciences: Visual observation of electric sparks on gypsum dunes". In: *Nature* 240.5377, pp. 143–144.

Kikuchi, K. and T. Endoh (1982). "Atmospheric electrical properties of volcanic ash particles in the eruption of Mt. Usu Volcano, 1977". In: *Journal of the Meteorological Society of Japan* 1.60, pp. 548–561.

Klačka, J and M Kocifaj (2007). "Scattering of electromagnetic waves by charged spheres and some physical consequences". In: *Journal of Quantitative Spectroscopy and Radiative Transfer* 106.1, pp. 170–183.

Klacka, J and Miroslav Kocifaj (2010). "On the scattering of electromagnetic waves by a charged sphere". In: *Progress In Electromagnetics Research* 109, pp. 17–35.

Kocifaj, Miroslav, Gorden Videen, and Jozef Klačka (2015). "Backscatter in a cloudy atmosphere as a lightning-threat indicator". In: *Journal of Quantitative Spectroscopy and Radiative Transfer* 150, pp. 175–180.

Lacks, Daniel J. (2012). "The Unpredictability of Electrostatic Charging". In: *Angewandte Chemie International Edition* 51.28, pp. 6822–6823.

Lacks, Daniel J. and Artem Levandovsky (2007). "Effect of particle size distribution on the polarity of triboelectric charging in granular insulator systems". In: *Journal of Electrostatics* 65.2, pp. 107–112.

Lacks, Daniel J. and R. Mohan Sankaran (2011). "Contact electrification of insulating materials". In: *Journal of Physics D: Applied Physics* 44.45, p. 453001.

Lal, Surbhi, Stephan Link, and Naomi J Halas (2007). "Nano-optics from sensing to waveguiding". In: *Nature photonics* 1.11, pp. 641–648.

Larson, Kristine M (2013). "A new way to detect volcanic plumes". In: *Geophysical Research Letters* 40.11, pp. 2657–2660.

Larson, Kristine M et al. (2017). "Detection of plumes at Redoubt and Etna volcanoes using the GPS SNR method". In: *Journal of Volcanology and Geothermal Research*.

Lazebnik, Mariya et al. (2007). "A large-scale study of the ultrawideband microwave dielectric properties of normal, benign and malignant breast tissues obtained from cancer surgeries". In: *Physics in medicine and biology* 52.20, p. 6093.

McNutt, Stephen R. and Earle R. Williams (2010). "Volcanic lightning: global observations and constraints on source mechanisms". In: *Bulletin of Volcanology* 72.10, pp. 1153–1167.

Méndez Harper, Joshua and Josef Dufek (2015). "The Electrification of Volcanic Particles during the Brittle Fragmentation of the Magma Column". In: *Proc. ESA Annual Meeting on Electrostatics 2015*.

— (2016). "The effects of dynamics on the triboelectrification of volcanic ash". In: *Journal of Geophysical Research: Atmospheres*, 2015JD024275.

Mendez Harper, Joshua et al. (2017). "Electrification of sand on Titan and its influence on sediment transport". In: *Nature Geoscience*.

Mie, Gustav (1908). "Contributions to the optics of turbid media, particularly of colloidal metal solutions". In: *Contributions to the optics of turbid media, particularly of colloidal metal solutions Transl. into ENGLISH from Ann. Phys.(Leipzig), v. 25, no. 3, 1908 p 377-445*.

Miura, Toshiro, Takehiro Koyaguchi, and Yoshikazu Tanaka (1996). "Atmospheric electric potential gradient measurements of ash clouds generated by pyroclastic flows at Unzen Volcano, Japan". In: *Geophysical Research Letters* 23.14, pp. 1789–1792.

— (2002). "Measurements of electric charge distribution in volcanic plumes at Sakurajima Volcano, Japan". In: *Bulletin of volcanology* 64.2, pp. 75–93.

Mizuno, Akira and Masumi Fukuma (1985). "Decrease in charge of sharp-edged ellipsoidal particles by self-discharge". In: *IEEE transactions on industry applications* 1, pp. 41–46.

Nagata, Takesi, Syuzo Sakuma, and Naoshi Fukushima (1948). "On the lava flow newly ejected from Sakurajima Volcano". In:

Nicora, Maria Gabriela et al. (2013). "Actividad eléctrica asociada a la erupción del complejo volcánico Cordón Caulle durante 2011". In: *www.scielo.ar*.

Oguchi, Tomohiro et al. (2009). "Measurements of dielectric constant of volcanic ash erupted from five volcanoes in Japan". In: *IEEE Transactions on Geoscience and Remote Sensing* 47.4, pp. 1089–1096.

Pahtz, T., H. J. Herrmann, and T. Shinbrot (2010). "Why do particle clouds generate electric charges?" In: *Nature Physics* 6.5, pp. 364–368.

Rowe, Jason F et al. (2008). "The Very Low Albedo of an Extrasolar Planet: MOST* Space-based Photometry of HD 209458". In: *The Astrophysical Journal* 689.2, p. 1345.

Schäfer, J, S-C Lee, and A Kienle (2012). "Calculation of the near fields for the scattering of electromagnetic waves by multiple infinite cylinders at perpendicular incidence". In: *Journal of Quantitative Spectroscopy and Radiative Transfer* 113.16, pp. 2113–2123.

Schimmer, O et al. (2007). "Instantaneous distinction between double and single frozen fish using a new handheld time domain reflectometer". In: *Proc. ISEMA*.

Sheen, NI and IM Woodhead (1999). "An open-ended coaxial probe for broad-band permittivity measurement of agricultural products". In: *Journal of Agricultural Engineering Research* 74.2, pp. 193–202.

Soh, Siowling et al. (2012). "Contact de-electrification of electrostatically charged polymers". In: *Journal of the American Chemical Society* 134.49, pp. 20151–20159.

Symons, G. J. (George James) et al. (1888). *The eruption of Krakatoa, and subsequent phenomena*. London, Trübner & co.

Thiessen, Elena et al. (2014). "Infrared light extinction by charged dielectric core-coat particles". In: *The European Physical Journal D* 68.4, p. 98.

Thomas et al. (2007). "Electrical Activity During the 2006 Mount St. Augustine Volcanic Eruptions". In: *Science* 315.5815, pp. 1097–1097.

Thomas et al. (2009). "Characterisation of electrostatic properties of powder coatings in relation with their industrial application". In: *Powder Technology*. Selection of Papers

from the Symposium Powder Science and Technology - Powders and Sintered Material STP-PMF 2007Symposium on Powder Science and Technology - Powders and Sintered Material STP-PMF 2007 190.1–2, pp. 230–235.

Van Eaton, Alexa R. et al. (2016). "Volcanic lightning and plume behavior reveal evolving hazards during the April 2015 eruption of Calbuco volcano, Chile". In: *Geophysical Research Letters* 43.7, 2016GL068076.

Wang, Neng, Shiyang Liu, and Zhifang Lin (2013). "Tailoring optical properties of surface charged dielectric nanoparticles based on an effective medium theory". In: *Optics express* 21.17, pp. 20387–20393.

Xie, L. et al. (2016). "Effect of humidity on contact electrification due to collision between spherical particles". In: *AIP Advances* 6.3, p. 035117.